General Disclaimer

One or more of the Following Statements may affect this Document

- This document has been reproduced from the best copy furnished by the organizational source. It is being released in the interest of making available as much information as possible.

- This document may contain data, which exceeds the sheet parameters. It was furnished in this condition by the organizational source and is the best copy available.

- This document may contain tone-on-tone or color graphs, charts and/or pictures, which have been reproduced in black and white.

- This document is paginated as submitted by the original source.

- Portions of this document are not fully legible due to the historical nature of some of the material. However, it is the best reproduction available from the original submission.

Produced by the NASA Center for Aerospace Information (CASI)

A FINITE VOLUME METHOD FOR CALCULATING TRANSONIC POTENTIAL FLOW AROUND WINGS FROM THE PRESSURE MINIMUM INTEGRAL

Albrecht Eberle

1. Report No. NASA TM-75324	2. Government Accession No.	3. Recipient's Catalog No.
4. Title and Subtitle A FINITE VOLUME METHOD FOR CALCULATING TRANSONIC POTENTIAL FLOW AROUND WINGS FROM THE PRESSURE MINIMUM INTEGRAL		5. Report Date July, 1978
		6. Performing Organization Code
7. Author(s) Albrecht Eberle Messerschmitt-Bölkow-Blohm GMBH Ottorbrunn near Munich, West Germany		8. Performing Organization Report No.
		10. Work Unit No.
9. Performing Organization Name and Address Leo Kanner Associates Redwood City, California 94036		11. Contract or Grant No. NASw-2790
		13. Type of Report and Period Covered
12. Sponsoring Agency Name and Address National Aeronautics and Space Administration, Washington, D.C, 20546		Translation
		14. Sponsoring Agency Code

15. Supplementary Notes

Translation of "Eine Methode der finiten Volumen zur Berechnung der transsonischen Potentialströmung um Flügel aus dem Druckminimumintegral," Messerschmitt-Bölkow-Blohm Internal Report, Report No. MBB-UFE1407(Ö), February 27, 1978, 70 pages

16. Abstract

In contrast to the usual difference equations, analysis of the pressure minimum integral in the calculation of three-dimensional potential flow around wings makes it possible to use non-rectangular mesh networks for distributing the three-dimensional potential into discrete points so that preliminary pictures can be dispensed with and the method can be comparatively easily expanded to the treatment of realistic airplane configurations. Moreover, this method does not require the limit condition to be explicitly fulfilled, since it automatically results in the course of the calculation.
Thanks to the careful choice of items in the preliminary two-dimensional studies already carried out in conjunction with the concept of artificial viscosity, shock-pressure affected pressure distributions on any wings can be determined with accuracy using this method and requiring relatively short computer time.

17. Key Words (Selected by Author(s))	18. Distribution Statement
	Unclassified-Unlimited

19. Security Classif. (of this report)	20. Security Classif. (of this page)	21. No. of Pages	22. Price
Unclassified	Unclassified	63	

a	auxiliary variable
b	wing span
B	range, force of inertia
c	constant
C	solid surface
D	image determinant, "thickness"
e	importance function
ϵ	viscosity parameter, small sphere
η	image coordinate
f	function
ϕ	potential
Φ	disturbance potential
G	form function
Γ	circulation
H	hyperbolic (auxiliary) point
i	counting index
K	wake
κ	adiabatic exponent
L	corridor
M	Mach number
m	mass, "middle"
n	edge perpendicular
O	surface element
o	"top", "zero" and "dynamic air pressure"
P	pressure force, check point
p	pressure
q	total velocity
r	radius
ρ	density
s	path distance
u,v,w	velocity components
x	coordinate
X	auxiliary function

ξ	image coordinate	
y	coordinate	/v
Y	auxiliary function	
z	coordinate	
Z	auxiliary function	
ζ	image coordinate	
*	"sound"	

List of Figures

Table of Contents

A FINITE VOLUME METHOD FOR CALCULATING TRANSONIC POTENTIAL FLOW AROUND WINGS FROM THE PRESSURE MINIMUM INTEGRAL

Albrecht Eberle
Messerschmitt-Bölkow-Blohm GmbH, Ottorbrunn near Munich,
West Germany

1. Introduction

The development of a successful finite element method for calculating transonic flow around a profile [1] provided the precondition for programming this method.

In contrast to the usual difference methods, finite volume methods do not require a rectangular mesh network so that they are particularly suitable for treating complex aerodynamic configurations. Even if this paper only covers airfoil wing calculations in the case of transonic oncoming flow, naturally one has in the back of one's mind the intention of expanding the computer program in the above direction when the occasion arises.

The introduction of an extremely simply formulated concept of plastic viscosity makes it possible to calculate shock-effected supercritical pressure distributions on any wings.

If, moreover, the distant field solution for supersonic flow is used, this offers the possibility of calculating pressure distributions for oncoming flow mach numbers even greater than one.

2. Fundamental Equations

If we assume frictionless stationary flow of an ideal gas, this can be described by the continuity equation

$$(\varrho u)_x + (\varrho v)_y + (\varrho w)_z = 0 \qquad (1)$$

---

* Numbers in the margin indicate pagination in the foreign text.

and the condition of irrotationality

$$u_z = w_x \qquad (2)$$

$$u_y = v_x \qquad (3)$$

$$v_z = w_y \qquad (4)$$

With uniform oncoming flow the energy carried with the fluid element is constant:

$$\frac{2\varkappa}{\varkappa-1} \frac{p}{\varsigma} + q^2 = \frac{2\varkappa}{\varkappa-1} \frac{p_o}{\varsigma_o} \qquad (5)$$

with $\qquad q^2 = u^2 + w^2$

The change of state is determined by the following isentrope:

$$\varkappa^{(\frac{\varsigma_o \delta}{\delta})} \; \varsigma_o d = d \qquad (6)$$

with the Mach number M defined as follows

$$\varkappa \frac{p}{\varsigma} = \frac{q^2}{M^2}$$

then by inserting this in Eq. (5) the squared speed becomes

$$q^2 = \frac{\varkappa p_o M^2}{\varsigma_o (1 + \frac{\varkappa-1}{2} M^2)} \qquad (7)$$

3. Standardization

The irrelevant constants in Eqs. (5), (6) and (7) can be eliminated by introducing a dimensionless velocity $\bar{q}$:

$$q^2 = \frac{2\varkappa}{\varkappa-1} \frac{p_o}{\varsigma_o} \; \bar{q}^2$$

Then Eq. (5) becomes

$$\frac{\rho_0 P}{P_0 \rho} + \overline{q}^2 = 1 \qquad (8)$$

and Eq. (7) becomes

$$\overline{q}^2 = \frac{M^2}{\frac{2}{\varkappa-1} + M^2} \qquad (9)$$

Eq. (6) in (8) gives us:

$$\rho = \rho_0 \, (1 - \overline{q}^2)^{\frac{1}{\varkappa-1}} \qquad (10)$$

From Eq. (9) we read the standardized sound velocity as

$$\overset{\bullet}{q}^2 = \frac{\varkappa-1}{\varkappa+1}$$

If the undeleted variables are now understood to be the appropriately standardized variables, equations (1), (2), (3) and (4) remain unchanged.

4. Distant Field Solution

4.1 Prandtl Transformation

The flow behavior far downstream from the wing can be determined by the approximate solution of Eq. (1) for $x^2 + y^2 + z^2 \rightarrow \infty$. In this regard, Eq. (1) is differentiated out and in so doing the transverse velocity components with respect to u are ignored.

$$u\rho_x + \rho(u_x + v_y + w_z) = 0 \qquad (11)$$

the term ρ_x is determined by Eq. (10) with back differentiation:

3

$$u\varrho_x \approx q\varrho_{q^2}\; q^2{}_x = -\frac{2\varrho\, q^2\, q_x}{(\varkappa-1)\,(1-q^2)}$$

The squared velocity is replaced by Eq. (9):

$$u\varrho_x \approx - M^2 \varrho\, u_x$$

If we make the following approximate assumption that $M \simeq M_\infty$, then Eq. (11) becomes:

$$(1 - M_\infty^2)\, u_x + v_y + w_z = 0 \tag{12}$$

As a secondary condition, Eqs. (2), (3) and (4) have to be fulfilled. This a accomplished by introducing a potential according to the following specification:

$$u = \phi_x, \quad v = \phi_y, \quad w = \phi_z \tag{13}$$

as a result of which Eq. (12) assumes the following form:

$$(1 - M_\infty^2)\, \phi_{xx} + \phi_{yy} + \phi_{zz} = 0$$

If we transform the y and z axes with

$$\eta = \sqrt{1 - M_\infty^2}\; y, \quad \zeta = \sqrt{1 - M_\infty^2}\; z \tag{14}$$

then the Laplace equation becomes

$$\phi_{xx} + \phi_{\eta\eta} + \phi_{\zeta\zeta} = 0 \tag{15}$$

4

If we insert the equation

$$\phi = u_\infty x + \frac{w_\infty \zeta + v_\infty \eta}{\sqrt{1 - M_\infty^2}} + \varphi \tag{16}$$

for a turbulent parallel main flow into Eq. (15), then obviously the following equation must be solved:

$$\varphi_{xx} + \varphi_{\eta\eta} + \varphi_{\zeta\zeta} = 0 \tag{17}$$

To this end, Eq. (17) is multiplied by an importance function e and partially integrated over the region of flow, taking into consideration the boundary shown in the sketch below:

η = constant

$$\overline{\iiint_{(B)-KL\epsilon}} e\,(\varphi_{xx} + \varphi_{\eta\eta} + \varphi_{\zeta\zeta})\,dx\,d\eta\,d\zeta =$$

$$= \oiint_{CK_\infty L\epsilon} e\varphi_n\,dO - \iiint_{(B)-KL\epsilon} (e_x\varphi_x + e_\eta\varphi_\eta + e_\zeta\varphi_\zeta)\,dx\,d\eta\,d\zeta = 0 \tag{18}$$

If we replace e with Φ, we similarly obtain:
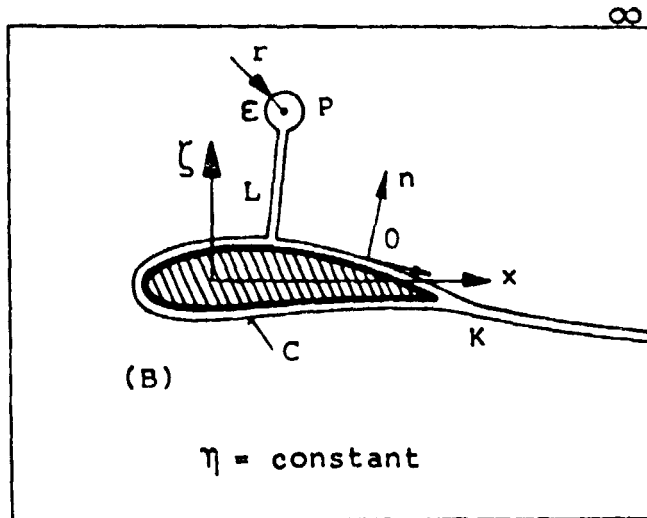
$$\underset{(B)-KL\mathcal{E}}{\iiint} \varphi(e_{xx} + e_{\eta\eta} + e_{\zeta\zeta})\, dx\, d\eta\, d\zeta =$$

$$= \underset{CK_\infty L\mathcal{E}}{\oiint} \varphi\, e_n\, dO - \underset{(B)-KL\mathcal{E}}{\iiint} (e_x \varphi_x + e_\eta \varphi_\eta + e_\zeta \varphi_\zeta)\, dx\, d\eta\, d\zeta$$

The volume integral on the right side is replaced by Eq. (18):

$$\underset{CK_\infty L\mathcal{E}}{\oiint} (\varphi\, e_n - e\varphi_n)\, dO = \underset{(B)-KL\mathcal{E}}{\iiint} \varphi(e_{xx} + e_{\eta\eta} + e_{\zeta\zeta})\, dx\, d\eta\, d\zeta$$

According to the definition and taking into consideration Eq. (16) the normal derivative Φ_n and the disturbance potential Φ disappear at infinity.

On the corridor L the derivatives for outgoing flight and return flight cancel each other out so that their contribution disappears.

In the wake K, the normal derivatives of the disturbance potential indeed cancel each other out, since there is a steady velocity field, but a potential difference between the top and bottom side should be allowed in order to simulate the departing vortex layer. This thus leaves us with the following equation from the integral equation:

$$\underset{\mathcal{E}}{\oiint} \varphi\, e_n\, dO = \underset{\mathcal{E}}{\oiint} e\, \varphi_n\, dO + \underset{C}{\oiint} (e\, \varphi_n - \varphi\, e_n)\, dO - \underset{K}{\iint} \varphi\, e_n\, dO$$

$$+ \underset{(B)-\mathcal{E}K}{\iiint} \varphi(e_{xx} + e_{yy} + e_{zz})\, dx\, d\eta\, d\zeta$$

6

The left integral can be evaluated immediately if ε represents the surface of a small sphere and e is exclusively a function of the radius. Then Φ tends towards the value Φ_p, and $\delta/\delta r$ becomes $\delta/\delta r$, with the integrand becoming a constant:

$$\oiint_{\varepsilon} \varphi e_n dO = \varphi_p e_r \oiint_{\varepsilon} dO = \varphi_p e_r \; 4 \pi r^2$$

If we now call for

$$e_r \; 4 \pi r^2 = 1$$

it follows that

$$e = - \frac{1}{4 \pi r}$$

If we insert this result into the integral equation and let ε shrink to 0, we finally obtain:

$$\varphi_P = \frac{1}{4\pi} \left[\oiint_{C+K} \varphi \left(\frac{1}{r} \right)_n \; dO - \oiint_{C} \frac{\varphi_n}{r} \; dO \right] \tag{19}$$

4.3 Displacement Term

We are looking for an approximate solution of the second integral of Eq. (19) for a wing of moderate thickness. Then the following simplifications are valid:

$$dO = dx d\eta = dx \sqrt{1 - M_\infty^2} \; dy$$

$$\frac{\partial}{\partial n} = \frac{\partial}{\partial \zeta} = \frac{\partial}{\sqrt{1 - M_\infty^2} \; \partial z} \qquad \text{(from (14))}$$

$$\succ \varphi_D = - \frac{1}{4\pi} \oiint_{C} \frac{\varphi_z}{r} \; dxdy$$

For small excess velocities the linearized limit condition

$$\varphi_z = u_\infty \frac{dz}{dx}$$

can be used, with which the partial integral can be integrated as follows:

$$\varphi_D = -\frac{u_\infty}{4\pi} \left[\int \frac{\Delta z}{r} \Big|_{front}^{rear} \, dy - \int \oint z \, (\frac{1}{r})_x \, dxdy \right]$$

The first term does not apply in the case of closed profile sections. Also, far downstream from the wing the effect of singularities appears punctiform so that ultimately we arrive at the following final result:

$$\varphi_D = \frac{u_\infty}{4\pi} \int \frac{x_P - x_m}{\left\{ (x_P-x_m)^2 + (1-M_\infty^2)\left[(y_P-y_m)^2 + (z_P-z_m)^2 \right] \right\}^{3/2}}$$
$$\cdot \oint_{section} z\,dx \cdot dy \tag{20}$$

The integrations are performed numerically in section.

4.4 Vortex Term

The first integral from Eq. (19) can be evaluated as follows using appropriate linearizations:

$$\varphi_\Gamma = \frac{1}{4\pi} \oiint_{C+K} \varphi \, (\frac{1}{r})_n \, d0 \approx$$

$$\approx -\frac{1}{4\pi} \iint_{C+K} (\varphi_o - \varphi_u) \, (\frac{1}{r})_{\zeta_P} \, dxd\eta =$$

8

$$= \frac{z_P}{4\pi} \int\limits_{-bo}^{b} \int\limits_{0}^{\infty} \frac{\Delta\varphi}{r^3}\, dx\,dy =$$

$$= -\frac{z_P}{4\pi} \int\limits_{-b}^{b} \int\limits_{0}^{\infty} \frac{\Delta\varphi\, d\,(x_P-x)\, dy}{\left\{(x_P-x)^2+(1-M_\infty^2)\left[(z_P-z)^2+(y_P-y)^2\right]\right\}^{3/2}}$$

$$= -\frac{z_P}{4\pi} \int\limits_{-b}^{b} \int\limits_{0}^{\infty} \frac{\Delta\varphi\left[a^2+(x_P-x)^2-(x_P-x)^2\right]\, d(x_P-x)\,dy}{\left[a^2+(x_P-x)^2\right]^{3/2}}$$

$$= -\frac{z_P}{4\pi} \int \frac{\Delta\varphi\,(x_P-x)}{a^2\sqrt{a^2+(x_P-x)^2}}\, \Bigg|_{m}^{\infty}\, dy$$

In these equations, because of the constancy of the velocities on the top and underside of the wake, the potential jump was assumed constant. We thus obtain:

$$\varphi_\Gamma = \frac{z_P}{4\pi} \int\limits_{-b}^{b} \frac{\Delta\varphi}{z_P^2+(y_P-y)^2}\, \cdot$$

$$\cdot \left\{ 1 + \frac{x_P-x_m}{\sqrt{(x_P-x_m)^2+(1-M_\infty^2)\left[(y_P-y)^2+(z_P-z_m)^2\right]}} \right\}\, dy \tag{21}$$

where the m line can be assumed to be at about 25% of the local chord length.

5. Continuity Equation Modification for Transonic Flow

5.1 Directional Dependence in the Case of Supersonic Flow

Without a provision to take into consideration the change in the type of flow at transonic velocities, a numerical algorithm

for solving continuity equation (1) would fail. Moreover, shock waves could not develop automatically in the course of the calculation. If we now want to determine the velocity potential at a special point P of the supersonic region, it must be borne in mind that the check point is influenced exclusively by physical data from the accompanying forward Mach cone.

It therefore suggests itself to coordinate the values ρu, ρv and ρw from Eq. (1) at a point H, which lies a small distance upstream from P, to the check point itself. This ensures that signals picked up downstream cannot reach the check point. In the case of subsonic flow, on the other hand, there is not directional dependency. Here the physical variables at the check point itself are used in the calculation. Accordingly, in the case of transonic flow, a numerical case distinction must be performed which depends on whether local supersonic or subsonic velocity is present.

5.2 Artificial Viscosity

The suggested assignment of physical quantities to check point P in the case of supersonic flow can be formulated mathematically by the linear upstream development of the variables ρu, ρv and ρw from Eq. (1). This should first of all be done for ρu:

$$(\rho u)_H = (\rho u)_P + (\rho u)_{PS} (S_H - S_P)$$

where S is at least approximately the run length along the flow line through P. The derivation $(\rho u)_S$ is formed as follows:

$$S_{(b\delta)} \frac{b}{n} + S_{(\frac{b}{n})} b\delta = S_{(\frac{b}{b} n\delta)} = S_{(n\delta)}$$

Since H is only a small distance from P, the flow line can be

approximated as a straight line so that $(u/q)_S$ disappears.

$$(\varrho u)_H = \varrho u + \frac{u}{q} (\varrho q)_S \, \Delta s$$

Since the local density must be computed in the computer program anyway, it is advisable to change over from S to ρ as the independent variable:

$$(\varrho q)_S \Delta s = (\varrho q)_\varrho \, \Delta \varrho$$

Differentiation with the help of Eqs. (10) and (9) gives us

$$(\varrho q)_S \Delta s = q \, (1 - \frac{1}{M^2}) \Delta \varrho \, .$$

For distinguishing the type of flow we can here comfortably introduce the switching function "max":

$$(\varrho u)_H = u \left[\varrho + \max \left(0, \, 1 - \frac{1}{M^2}\right) \, (\varrho_H - \varrho) \right]$$

For the terms ρv, ρw it is only necessary to replace u with v. A transonic computing process thus works if the following expression is merely placed in the check point for the density:

$$\varrho \longrightarrow \varrho + \max \left(0, \, 1 - \frac{1}{M^2}\right) \Delta \varrho$$

5.3 Viscosity Parameter

Since the vector length between auxiliary point H and check point P can be chosen more or less arbitrarily, the artificial viscosity is generalized by a parameter ε which is constant in the entire flow field:

$$\varrho \longrightarrow \varrho + \varepsilon \max \left(0, \, 1 - \frac{1}{M^2}\right) \Delta \varrho$$

Thus, on the one hand, the accuracy of the method can be increased (small ϵ), and on the other hand iterative convergence from case to case can be guaranteed (large ϵ).

6. The Variation Principle

6.1 The Euler Minimum Principle

Here we will try to put the continuity equation (1) in a form appropriate for the computer which does not allow the introduction of a nonperpendicular calculating mesh network. In this regard, in reference [1] a variation principle was derived from the weighted remainder and in reference [2] from the least square. An especially illuminating procedure is based on the Euler principle according to which the equilibrium of forces is formed on the fluid particle.
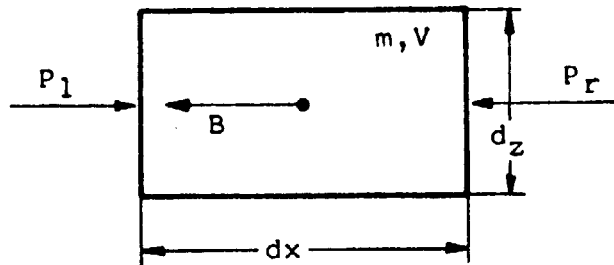
This should be done here first of all for the x-direction:

$$P_1 - B - P_r = 0$$

or

$$pdydz - m\dot{u} - (p + p_x dx)\, dydz = 0$$

$$p_x + \varrho\, \dot{u} = 0$$

In the case of stationary flow, the acceleration $\dot{u}$ can be written as follows independent of time:

$$\dot{u} = u_x \dot{x} + u_y \dot{y} + u_z \dot{z} = uu_x + vu_y + wu_z$$

With Eqs. (2)-(4), it follows that

$$p_x + \varrho(uu_x + vv_x + ww_x) = 0$$

The Euler mininum principle is based on elimination of the local derivation by using the chain rule

$$\frac{\partial}{\partial x} = \phi_x \frac{\partial}{\partial \phi}$$

$$\succ p_\phi + \varrho(uu_\phi + vv_\phi + ww_\phi) = 0 \tag{22}$$

This same equation is obtained if the equiblibrium of forces is formed in the y direction or z direction.

6.2 The Pressure Minimum Integral

That Eq. (22) satisfies the continuity equation can be seen if, similar to what we did in section 4.2, we partially integrate over the region of flow and in so doing Eq. (13) is taken into account:

$$\iiint p_\phi \, dxdydz + \iiint \varrho(u\phi_{x\phi} + v\phi_{y\phi} + w\phi_{z\phi}) \cdot dxdydz = 0$$

Thus the second integral obviously becomes

$$\oiint \phi_\phi \varrho u \, dydz - \iiint \phi_\phi(\varrho u)_x \, dxdydz$$
$$+ \oiint \phi_\phi \varrho v \, dxdz - \iiint \phi_\phi(\varrho v)_y \, dxdydz$$
$$+ \oiint \phi_\phi \varrho w \, dxdy - \iiint \phi_\phi(\varrho w)_z \, dxdydz$$
$$= \oiint \phi_\phi \varrho \vec{q} \cdot \vec{n} \, d0 - \iiint \phi_\phi \left[(\varrho u)_x + (\varrho v)_y + (\varrho w)_z\right] dxdydz$$

Now we can obviously see that

$$\phi_\phi = \frac{\partial \phi}{\partial \phi} = 1.$$

The second integral disappears because of Eq. (1), likewise the first integral, since first of all the kinematic flow conditions on the boundary of the body has to be satisfied and, secondly, the mass flow through the distant boundary must disappear. Thus the following simple result holds:

$$\iiint p\phi \; dxdydz = 0$$

or because of Eq. (22):

$$\iiint \varrho (uu\phi + vv\phi + ww\phi) \; dxdydz = 0$$

(23)

7. Numerical Evaluation

7.1 The Eight-Node Element Cube

To evaluate Eq. (23) we make use of the finite element method. In so doing, the potential is represented in a stepwise manner but continuously and without gaps in a three-dimensional mesh network.

A useful approximation for this is the trilinear element cube with the corner point coordinates in the Cartesian auxiliary coordinate system ξ, η, ζ according to the following table

i	ξ_i	η_i	ζ_i
1	1	-1	-1
2	-1	-1	-1
3	-1	1	-1
4	1	1	-1
5	1	-1	1
6	-1	-1	1
7	-1	1	1
8	1	1	1

A function f is then approximated in the cube including the sides
by the following equation

$$f = \frac{1}{8} \sum_1^8 f_i \, (1 + \xi_i \, \xi) \, (1 + \eta_i \, \eta) \, (1 + \zeta_i \, \zeta)$$

$$= \sum_1^8 f_i \, G_i \tag{24}$$

as one can easily convince oneself by trying it out or by
coefficient determination from the general equation.

7.2 The General Eight-Node Volume Element

The transition to a volume element with straight edges and
eight corners is made by successively replacing the function f
in Eq. (24) by x, y, z and ϕ, where now the coordinates ξ, η,
and ζ function as parameters:

$$x = \sum_1^8 x_i \, G_i$$

$$y = \sum_1^8 y_i \, G_i$$

$$z = \sum_1^8 z_i \, G_i$$

$$\phi = \sum_1^8 \phi_i \, G_i$$

To evaluate Eq. (23) we need the following derivations

$$u = \phi_x = \phi_\xi \, \xi_x + \phi_\eta \, \eta_x + \phi_\zeta \, \zeta_x$$
$$v = \phi_y = \phi_\xi \, \xi_y + \phi_\eta \, \eta_y + \phi_\zeta \, \zeta_y$$
$$w = \phi_z = \phi_\xi \, \xi_z + \phi_\eta \, \eta_z + \phi_\zeta \, \zeta_z$$

In this connection, the local derivations $\xi_{x,y,z}$, $\eta_{x,y,z}$ and $\zeta_{x,y,z}$ pose difficulties, since the approximation for x,y and z is not invertable. The problem can be solved, however, if first of all we write down the differentials of all the coordinates.

$$d\xi = \xi_x \, dx + \xi_y \, dy + \xi_z \, dz$$
$$d\eta = \eta_x \, dx + \eta_y \, dy + \eta_z \, dz$$
$$d\zeta = \zeta_x \, dx + \zeta_y \, dy + \zeta_z \, dz$$
$$dx = x_\xi \, d\xi + x_\eta \, d\eta + x_\zeta \, d\zeta$$
$$dy = y_\xi \, d\xi + y_\eta \, d\eta + y_\zeta \, d\zeta$$
$$dz = z_\xi \, d\xi + z_\eta \, d\eta + z_\zeta \, d\zeta$$

If we now substitue the differentials d_ξ, d_η, d_ζ of the three last equations by the right sides of the three first equations and in each case perform the coefficient comparison for dx, dy and dz, we obtain nine equations for the nine unknowns $\xi_{x,y,z}$, $\eta_{x,y,z}$ and $\zeta_{x,y,z}$. The time consuming but trivial solution leads to the following result:

$$\xi_x = \frac{(y_\eta z_\zeta - y_\zeta z_\eta)}{D}$$

$$\eta_x = \frac{(y_\zeta z_\xi - y_\xi z_\zeta)}{D}$$

$$\zeta_x = \frac{(y_\xi z_\eta - y_\eta z_\xi)}{D}$$

$$\xi_y = \frac{(x_\zeta z_\eta - x_\eta z_\zeta)}{D}$$

$$\eta_y = \frac{(z_\zeta x_\xi - z_\xi x_\zeta)}{D}$$

$$\zeta_y = \frac{(x_\eta z_\xi - z_\eta x_\xi)}{D}$$

$$\xi_z = \frac{(x_\eta\, y_\zeta - y_\eta\, x_\zeta)}{D}$$

$$\eta_z = \frac{(y_\xi\, x_\zeta - y_\zeta\, x_\xi)}{D}$$

$$\zeta_z = \frac{(x_\xi\, y_\eta - x_\eta\, y_\xi)}{D}$$

with
$$D = x_\xi\,(y_\eta\, z_\zeta - z_\eta\, y_\zeta) + y_\xi\,(z_\eta\, x_\zeta - x_\eta\, z_\zeta)$$
$$+ z_\xi\,(x_\eta\, y_\zeta - y_\eta\, x_\zeta)$$

7.3 The Element Pressure Minimum Integral

With the above operations we can now approximately evaluate
integral (23) for one element. To do this we use simple point
integration by forming the integrand at point

$$\xi = \eta = \zeta = 0$$

and the volume element is distorted with the image determinant
D derived in the previous section:

$$dxdydz \approx D \cdot \Delta\xi\, \Delta\eta\, \Delta\zeta = 8\, D$$

With the exception of an unimportant constant factor, Eq. (23)
is then expressed as follows if, for example, we differentiate
according to the potential for corner 1:

$$\iiint_E g\,(uu\phi_1 + vv\phi_1 + ww\phi_1)\; dxdydz \approx$$

$$c \cdot g\,\Big[(\phi_\xi\xi_x + \phi_\eta\eta_x + \phi_\zeta\zeta_x)\,(G_{1\xi}\,\xi_x + G_{1\eta}\,\eta_x + G_{1\zeta}\,\zeta_x)$$

$$+\; (\phi_\xi\xi_y + \phi_\eta\eta_y + \phi_\zeta\zeta_y)\,(G_{1\xi}\,\xi_y + G_{1\eta}\,\eta_y + G_{1\zeta}\,\zeta_y)$$

$$+\; (\phi_\xi\xi_z + \phi_\eta\eta_z + \phi_\zeta\zeta_z)\,(G_{1\xi}\,\xi_z + G_{1\eta}\,\eta_z + G_{1\zeta}\,\zeta_z)\Big]\,D$$

$$\text{for } \xi = \eta = \zeta = 0$$

By rearrangement we obtain a term of the following form for the integral:

$$\varrho(\phi_\xi\, x + \phi_\eta\, Y + \phi_\zeta\, z)$$

Finally, if we explicitly differentiate ϕ, we obtain

$$\varrho\sum_1^8 \phi_i\ (x\ G_{\xi_i} + Y\ G_{\eta_i} + z\ G_{\zeta_i})$$

7.4 The Global Pressure Minimum Integral /18

Now after the pressure minimum integral for an element with the pivot point marked "1" is evaluated, the construction of the entire volume integral no longer presents any difficulties. All that is necessary is for the contributions of all of the elements which contain the corner "1" to be counted together. So in the free field the contributions of eight elements, which have one and the same corner in common, are to be counted together, as one can easily imagine. Boundaries present no problems. Here, of course, in most cases less than eight elements are involved in the integrand. In general, four elements are involved.

7.5 Relaxation Method

So far we have treated Eq. (23) for the case of potential derivation at a selected mesh corner point. In order to solve Eq. (23) in a global association of elements, we start with the idea that the pressure minimum integral must disappear for each intersection of the mesh. Thus, from Eq. (23) we obtain just as many equations as unknown potential given values.

From this we can derive in a classical manner a relaxation method:

Up to a certain distance the flow field is completely covered with volume elements. The distant field solution of the potential as per Eqs. (16), (20) and (21) is specified on the distant field border. The tridiagonal matrix for the unknown potential values is set up along reasonably selected lines.

All contributions not stemming from this line are put on the right side. The resulting system of equations is solved directly. If we now move from line to line, we obtain an iterative algorithm with which the newest ϕ and ρ values are always used. In so doing, the flow field is repeatedly traversed until the potential values no longer change significantly.

Caution is necessary in determining the potential values on the top and bottom of the vortex layer. In this computer program, numerical stability was achieved as follows:

We define a mean potential as follows:

$$\phi_m = \frac{(\phi_o + \phi_u)}{2}$$

and determine the potential values on the top and bottom of the trailing edge of the wing ϕ_{oHK}, ϕ_{uHK}. Thus the constant potential jump $\Delta\phi = \phi_{oHK} - \phi_{uHK}$ along sections y = constant are assumed to be known. Now in order to calculate the potential values on both sides of the vortex layer, we first of all solve for ϕ_m and then form

$$\phi_o = \phi_m + \frac{\Delta\phi}{2}$$

$$\phi_u = \phi_m - \frac{\Delta\phi}{2}$$

NACA-0012 Wing

For the first test sample we used as a basis for the calculation a simple swept back wing with linear warping and a constant profile.

Fig. 1 shows the outer boundary belonging to each y section on which the distant field potential according to Eqs. (16), (20) and (21) is specified. The influences of the other half of the wing on the computation fields shown are also taken into consideration.

The wing is centered on an impenetrable wall so that even flows with small slideslip angles can be calculated with a very simplified fuselage effect. Beyond the wingtip the calculating network is expanded by another three sections which contain no solid contours. The vortex layer leaves the trailing edge in the direction of the local bisecting lines.

Figs. 2-16 show the pressure distributions. The points above the profile indicate the elements in which supersonic velocity prevails. The mark on the C_p axis represents the critical pressure coefficient for the total oncoming flow Mach number.

Fig. 18 requires more detailed explanation. The top side pressure distribution acts somewhat unevenly, since the shock front jumps along the wingspan a few times between the mesh coordinates.

In this as in all other shock capturing methods, the shock front can coincide only with network coordinates so that, in general, the Rankine-Hugoniot shock equation and the angle correlations in front of and behind the shock cannot be satisfied.

If one wanted to improve this, the method would be very complicated and would use an enormous amount of computer time. We can manage with this method by approximately anticipating all possible shock formations by means of a mesh construction perpendicular to the body. Even this is very difficult. It is simpler to concentrate the network in such a way that shocks can be geometrically approximated in steps. Because of a lack of computer time, no studies on this could be carried out.

The problem is most easily coped with by intensifying the artificial viscosity via the specifiable viscosity parameters. Then the result becomes almost independent of the "false" local network geometry in the vicinity of the shock.

Figs. 20-22 are auxiliary diagrams showing the coefficient distributions with respect to the local chord length. In these diagrams the pitching moment is formed around the forward most point of the wing. Using this, together with the lift distribution and position of the pressure point, we can convert the moment to any point of impact.

The iterative convergence is considerably accelerated through successive network divisions with subsequent potential interpolation. So for this example the result was obtained after eight minutes of computer time on the cnetral unit of an IBM 370/168. This required only 12 iterations per network (three altogether).

The computer time could be reduced even more considerably if greater access storage were available. In the absence of storage capacity, the network geometry and the transformation matrix for each element must now be calculated anew for each iteration. However, this is still cheaper than reading off this once determined data from an external and thus slow storage.

B10X / NLR Model

This is a design study for the wing of a modern transport
plane. Again the same data are supplied as in the previous
example.

In particular, Fig. 36 shows that obviously a well balanced
upper wing surface has been achieved, for the shock intensities
on the outer wing are very small. At about two-thirds of the
chord length (y = 11.75, Fig. 31) the pressure distribution of
the basic profile is satisfactorily represented.

This example with 12 wing sections for each 32 profile
points required the solution of 4,320 unknown potential values.
The computer time was five minutes on the central computer of the
IBM 370/168.

9. Summary

This paper demonstrates the operability of a new finite
volume method for calculating shock-affected flow around a wing.
Because of the chronic lack of computer time no calculations could
be carried out on the dense mesh network provided by the program
which would certainly have produced more accurate results.
Nevertheless, on the basic of earlier experiments, it is worth-
while to extend the program to wing-fuselage combinations in w
which, because of the complicated boundary geometry, the
advantages of the finite volume technique actually first come to
bear. For this taks, the usual difference methods are suitable
only to a limited extent, since they all require a strictly
perpendicular network which leads to a considerable amount of
interpolation on solid surfaces. For this reason and because of
the quicker iterative convergence, methods such as this one
should take on considerable importance in the future.

REFERENCES

1. Eberle, A., "A finite element method for calculating tran-   /vi
   sonic potential flow around profiles," MBB UFE1325(Ö),
   (1977).

2. Firchau, W., M. Laihad and B. Kiekebusch, "Geometric data
   for constructing the ZKP model wing," MBB-TN-HE212-9/77
   (1977).

3. Eberle, A., "Profile optimization for transonic flow using
   the method of finite elements and characteristics,"
   MBB UFE1362(Ö) (1977).

4. Jameson, A. and D.A. Caughey, "A finite volume method for
   transonic potential flow calculations," AIAA Paper No. 77-
   635 (1977).
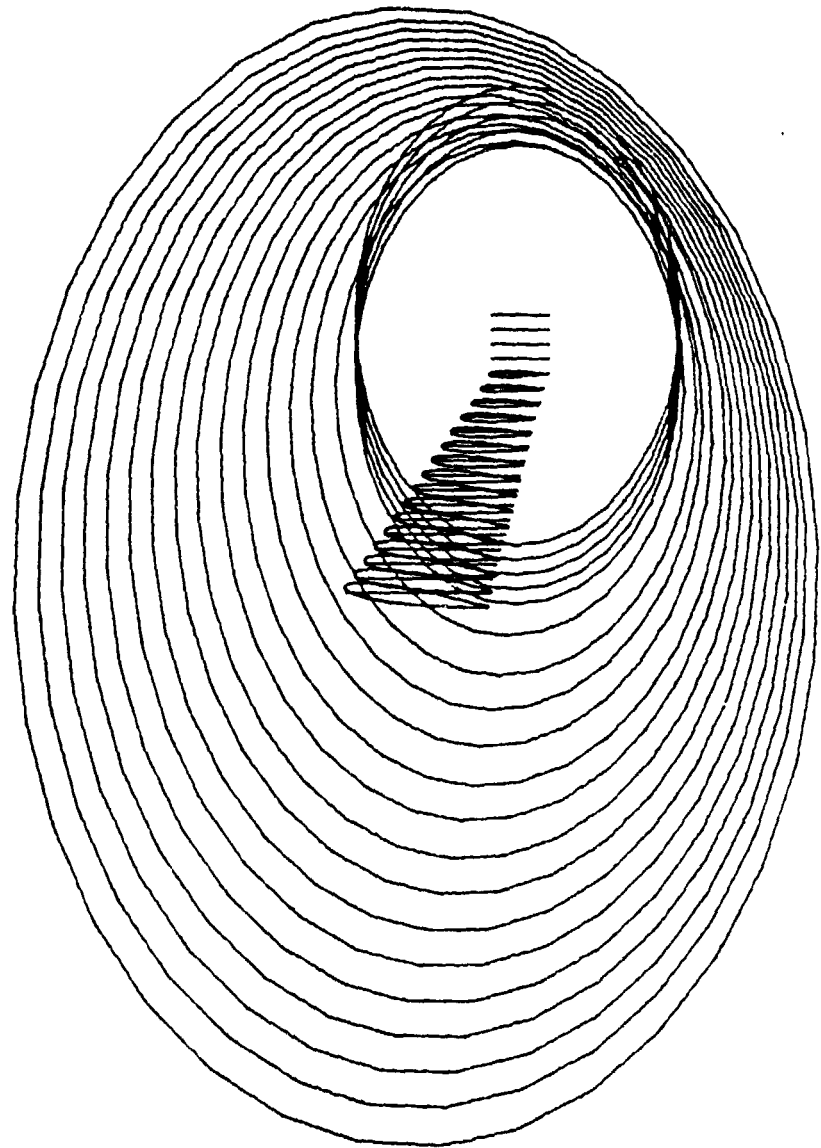
NACA 0012-   (wing)

(input)

Fig. 1
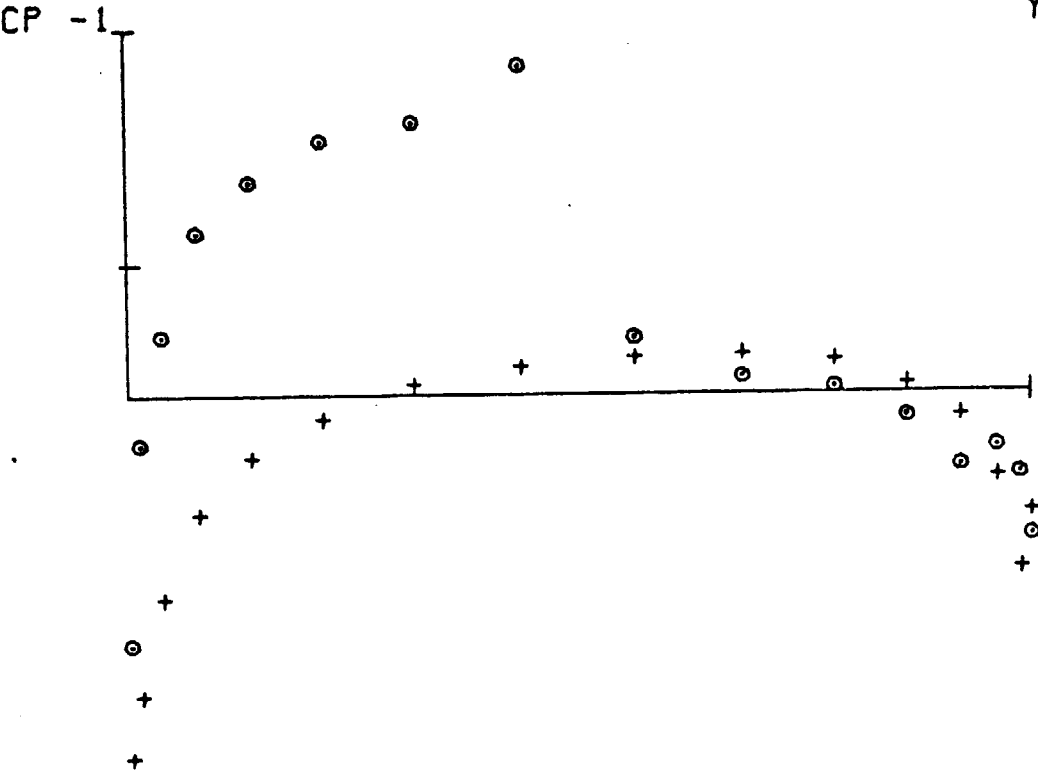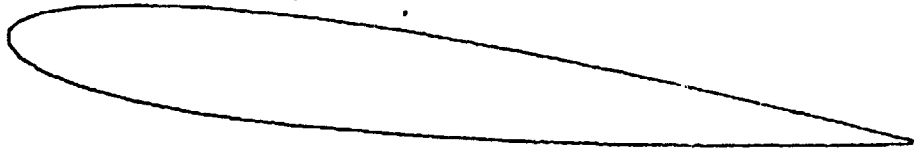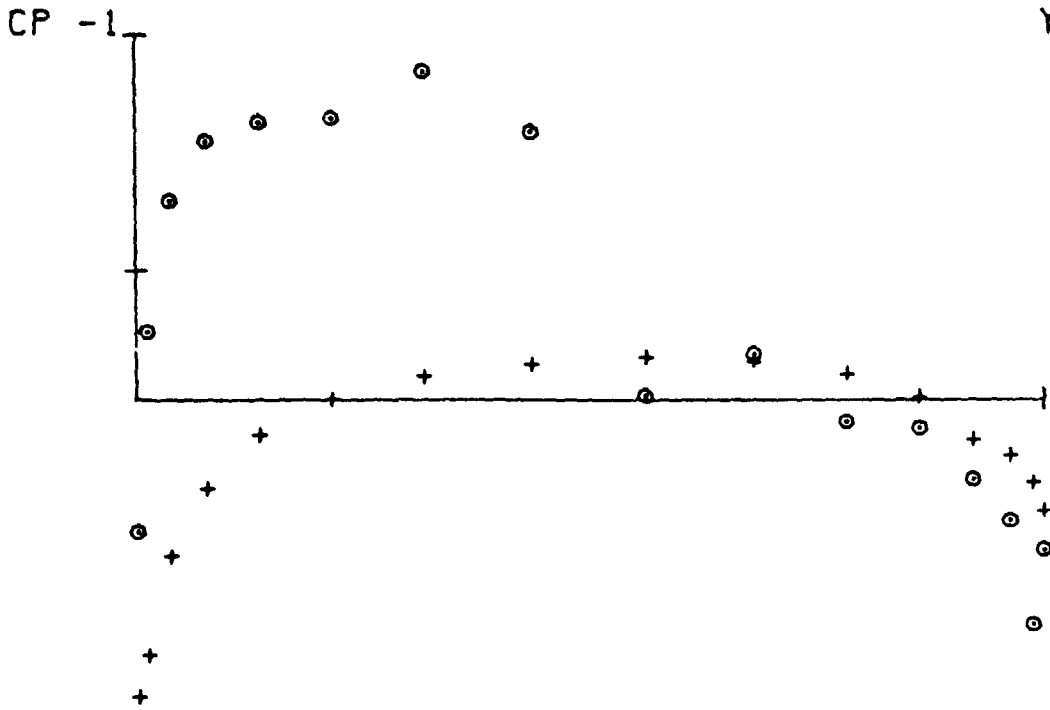
CP -1

Fig. 2

MBB

Fig. 3

26

CP -1

Y=25.000

Fig. 4

MBB

CP -1

Fig. 5

/30
Y=45.000

CP -1

Fig. 6

MBB

Fig. 7

MBB

Y=65.000

CP -1

Fig. 8

MBB

CP -1

Y=75.000

Fig. 9

MBB

Fig. 10

Y=95.000

CP -1

Fig. 11

CP -1

Y=105.000

Fig. 12

MBB

CP -1

Y=115.000

Fig. 13

MBB

CP -1

Y=125.000

Fig. 14

Y=135.000

CP -1

Fig. 15

MBB

CP -1
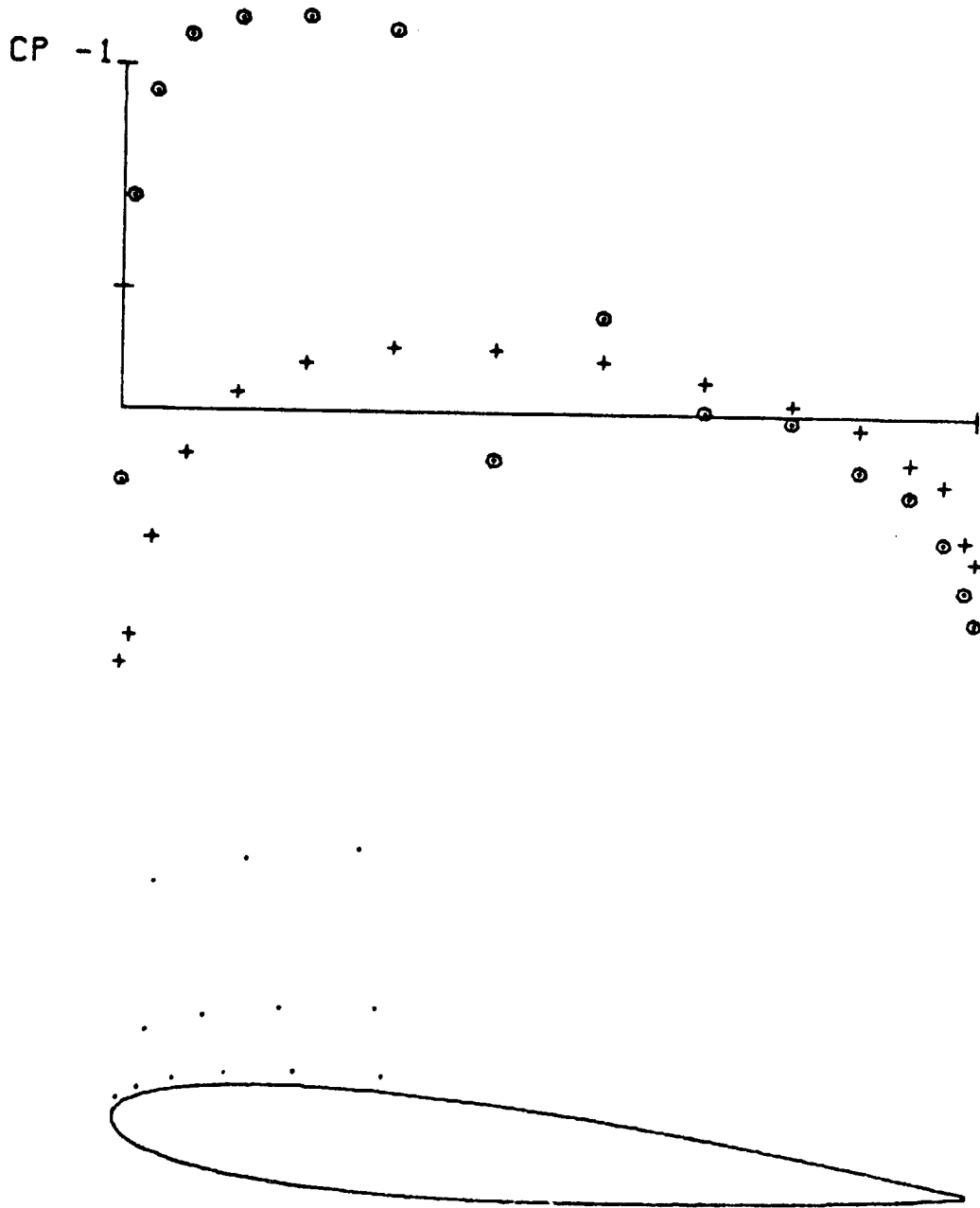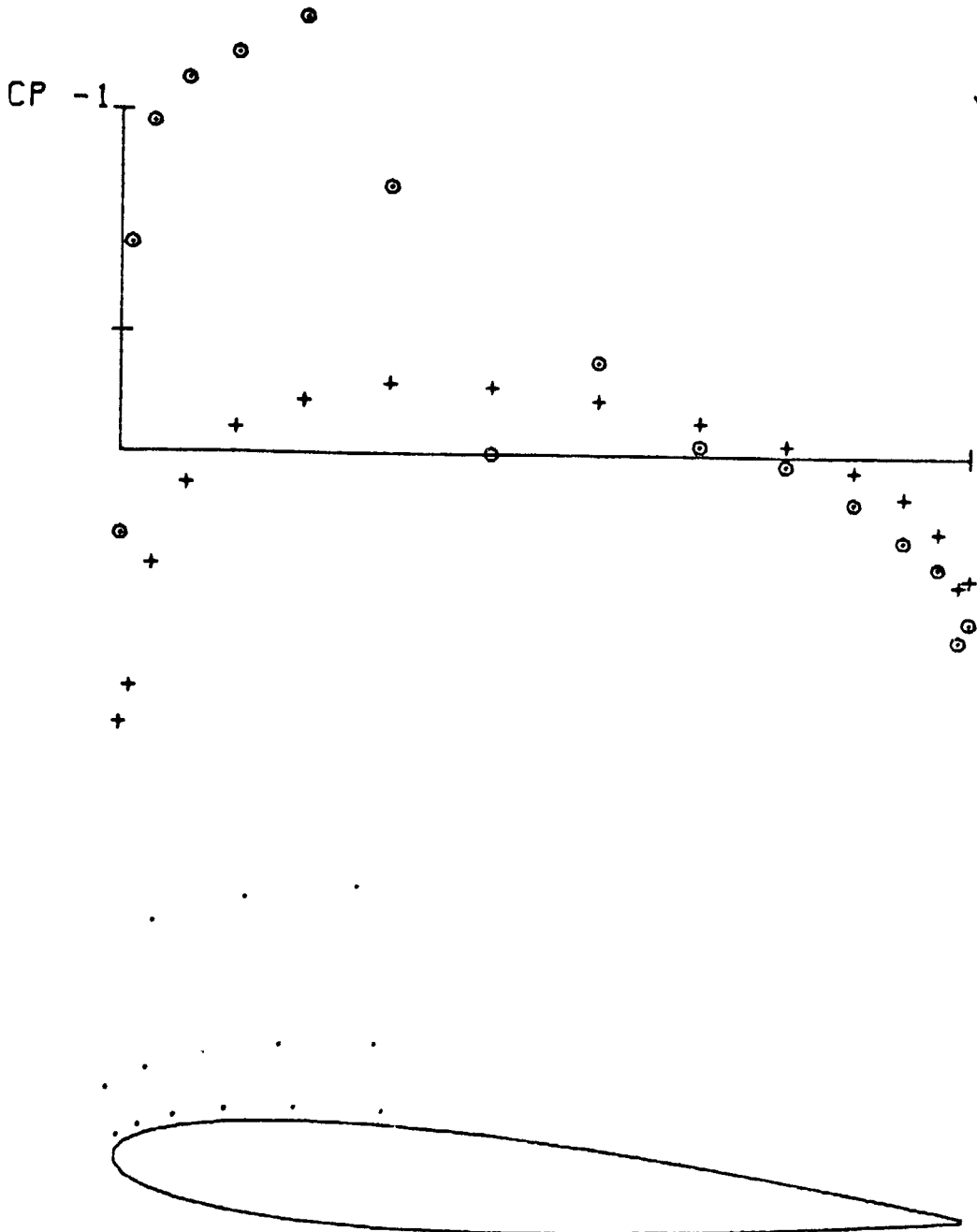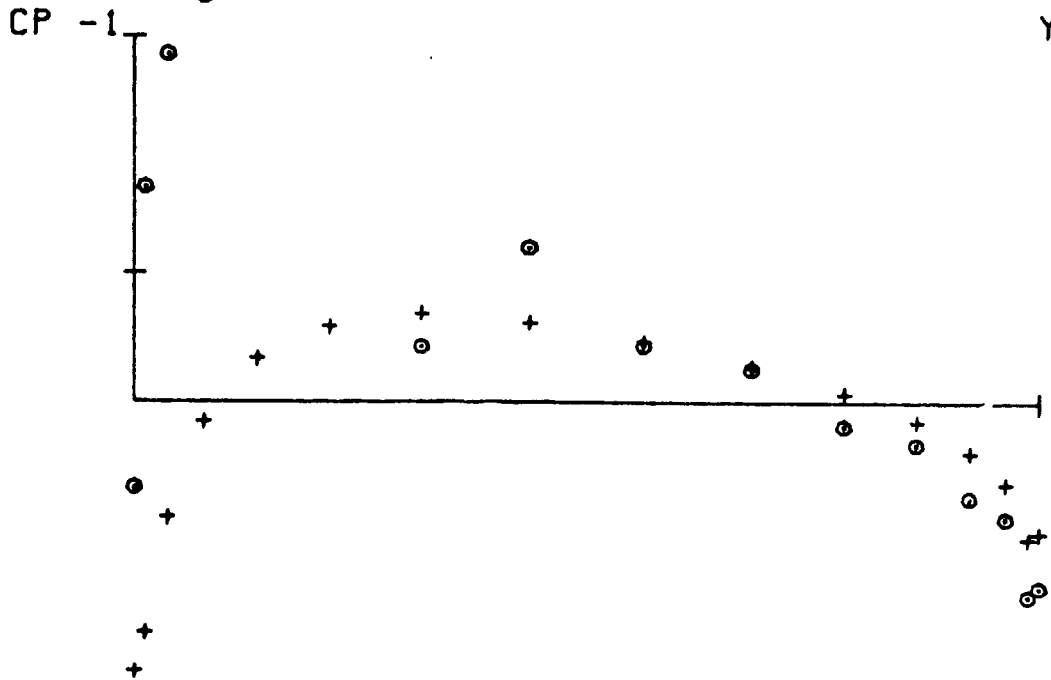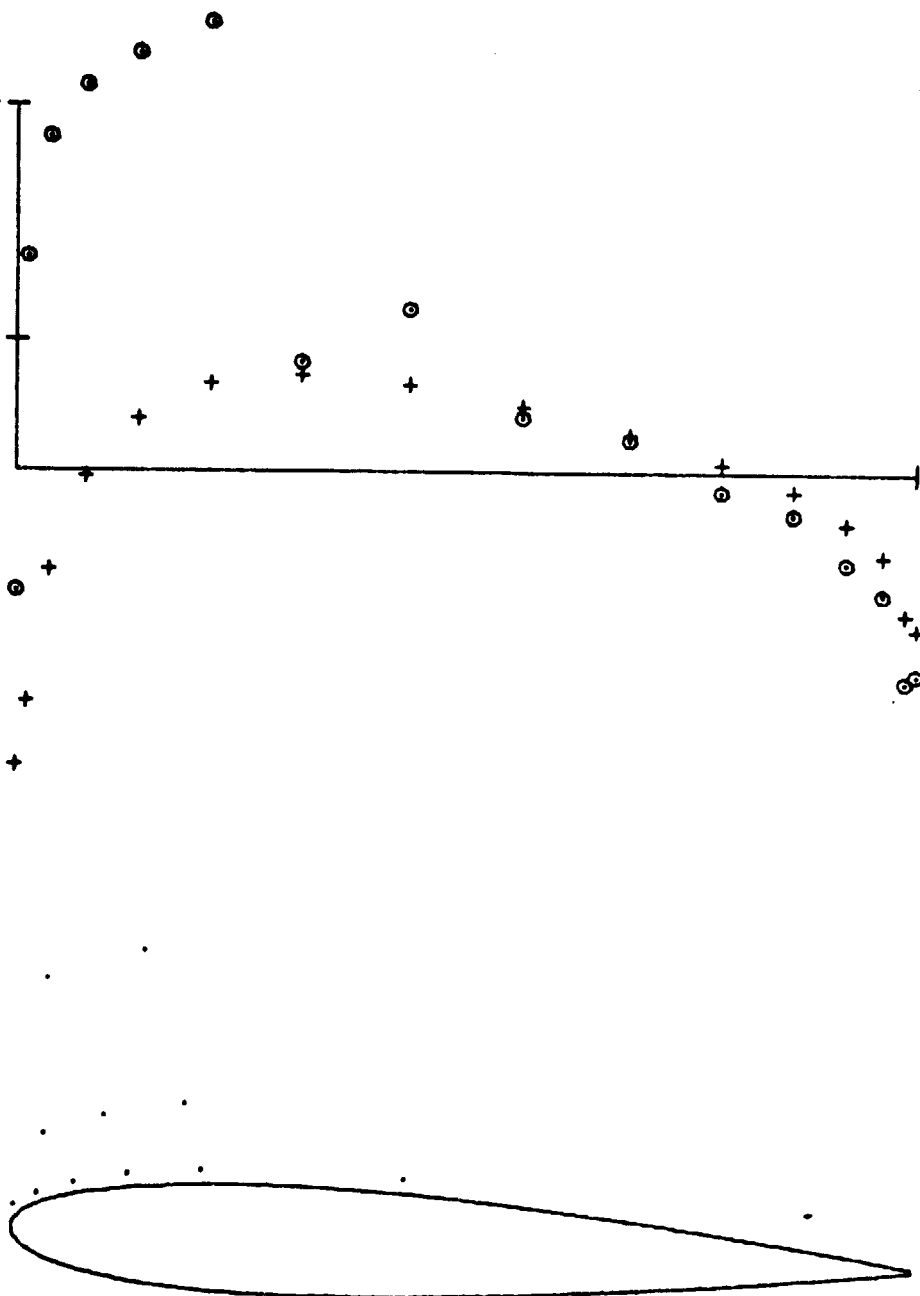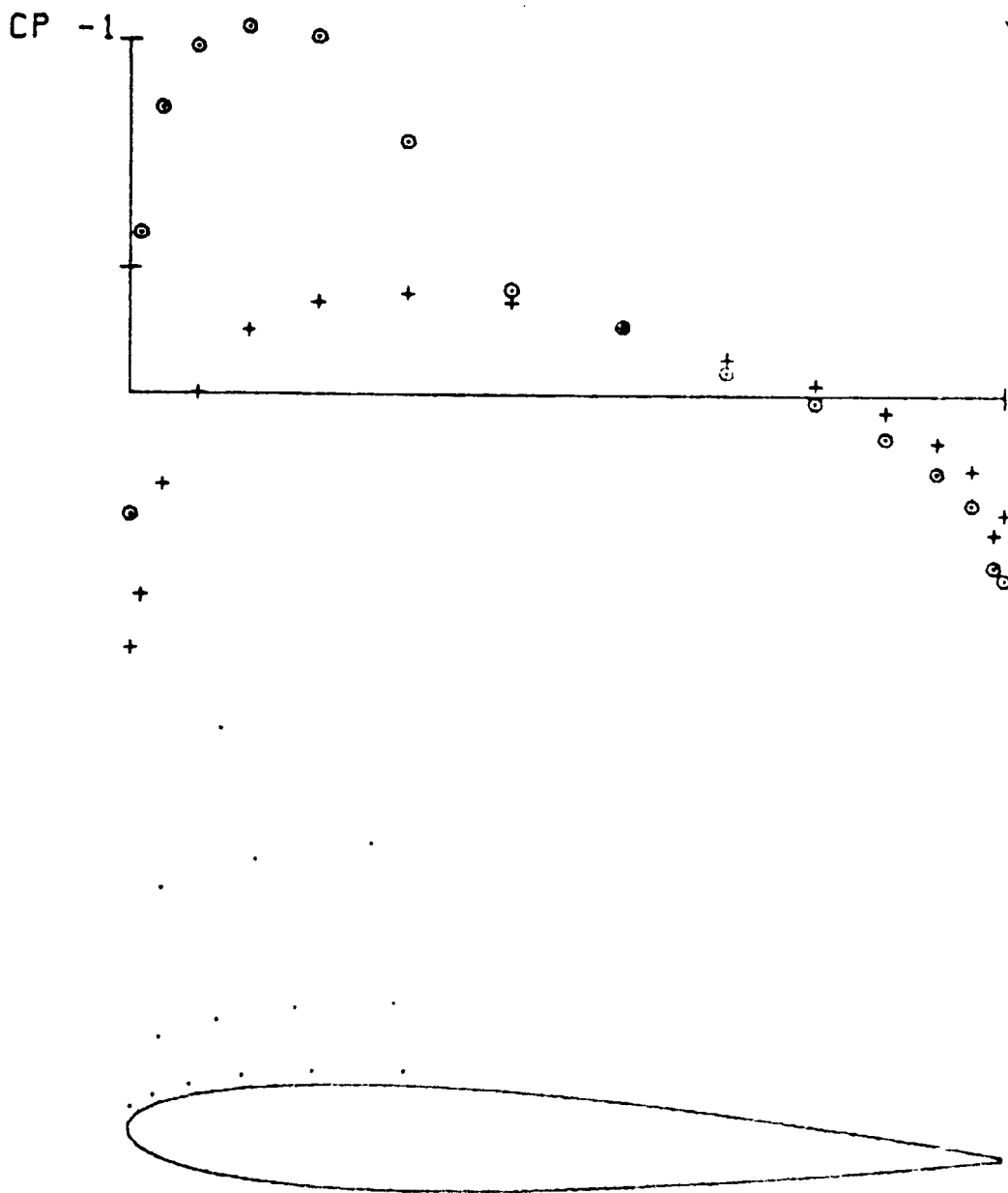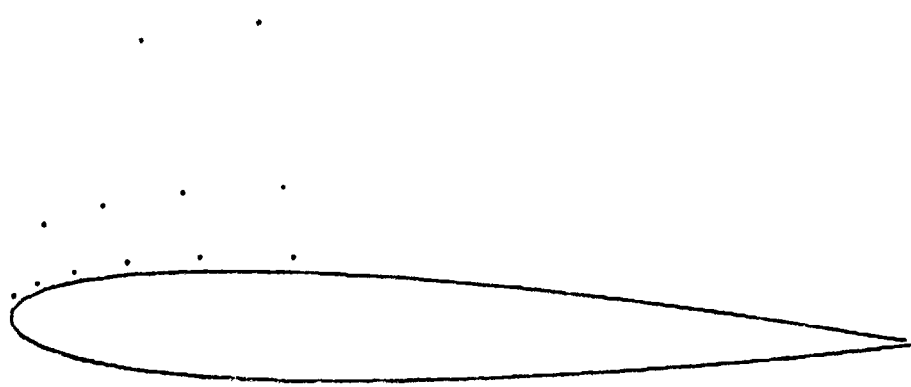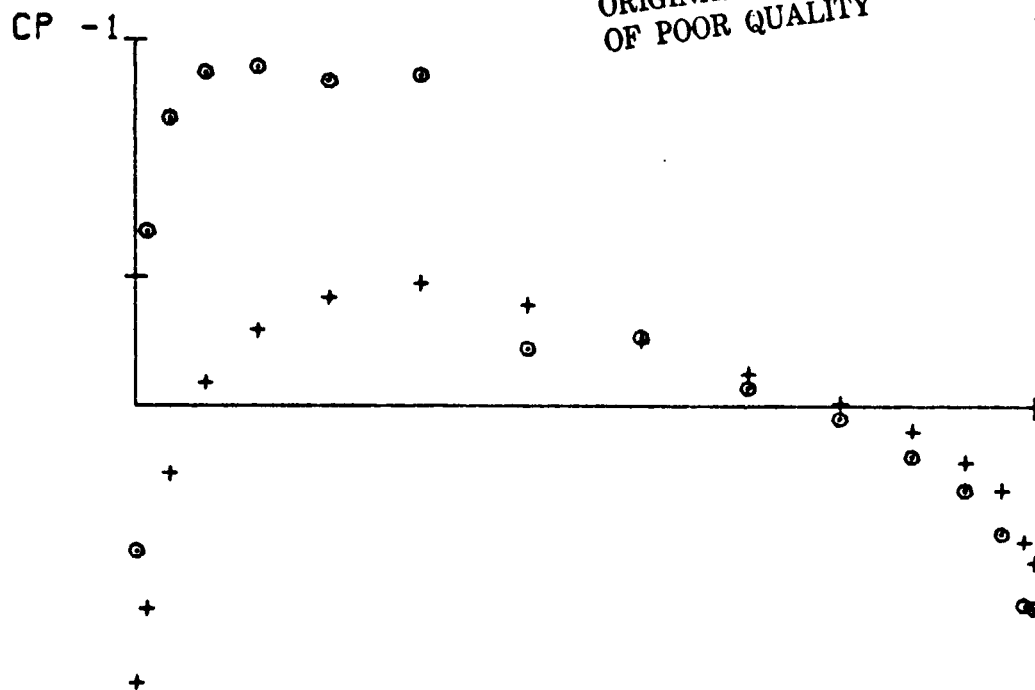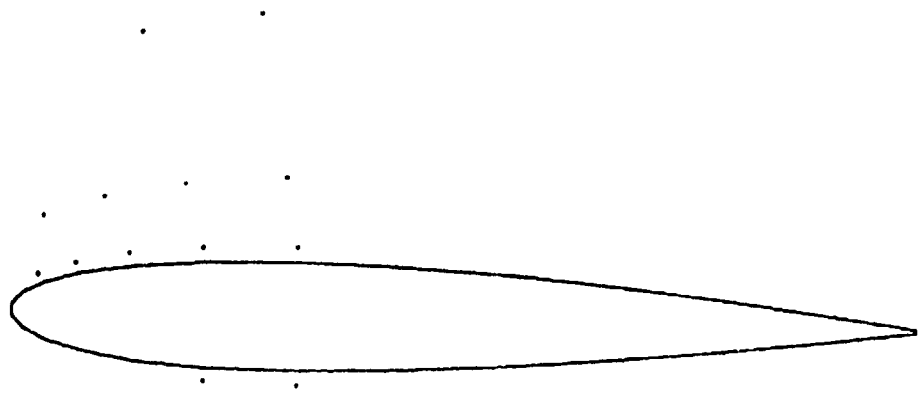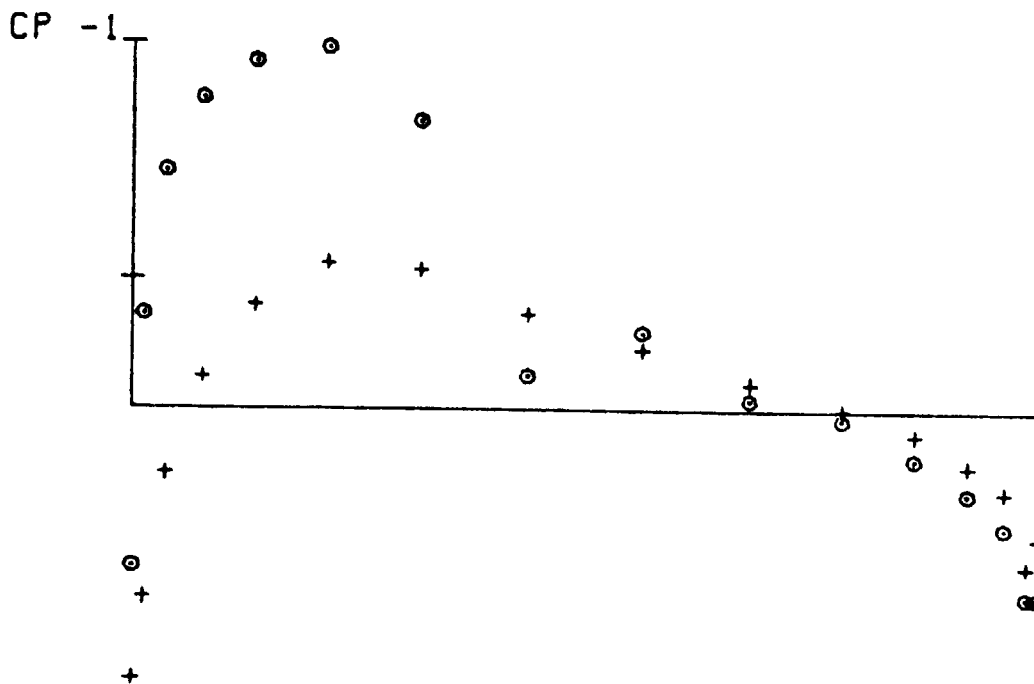
Y=145.000
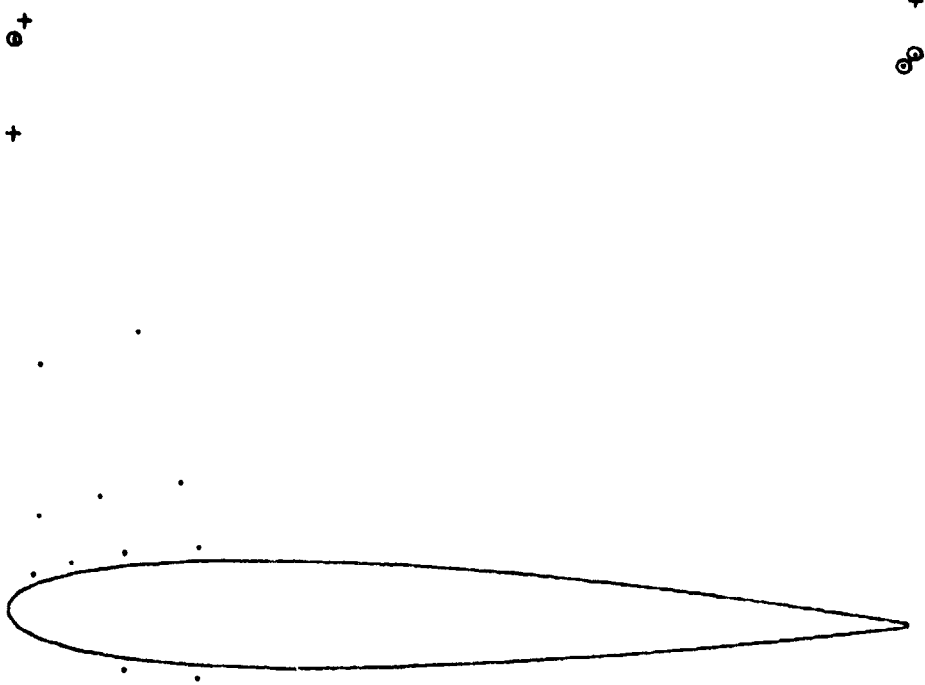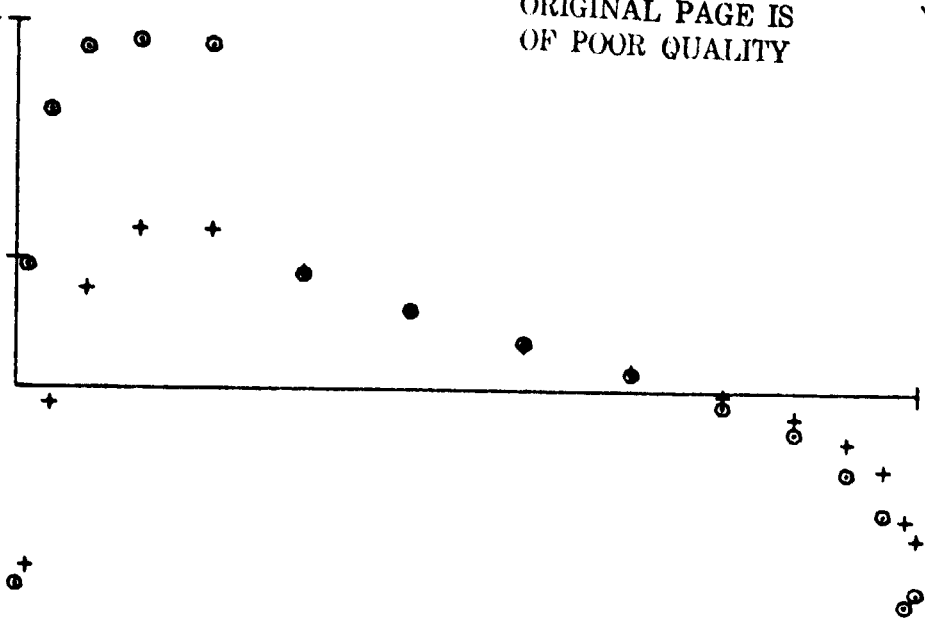
Fig. 16
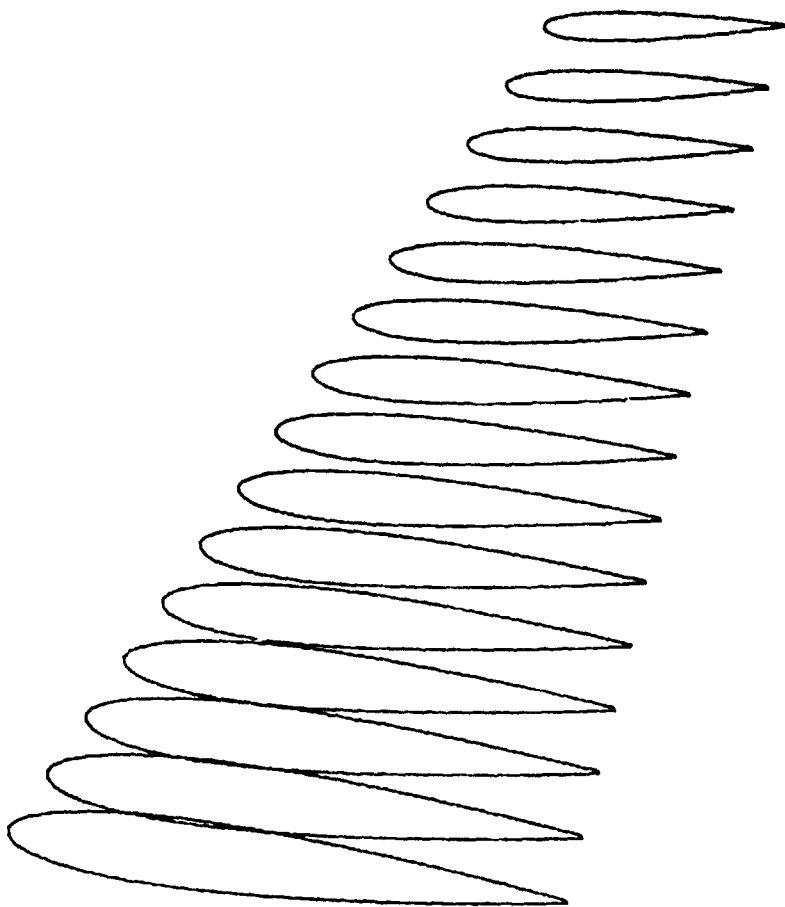
NACA 0012-FLUEGEL [wing]

MA=0.8300

AL=0.0   GRAD

BE=0.0   GRAD

CA=0.3112

CW=0.0166

CM=-0.2028

Fig. 17
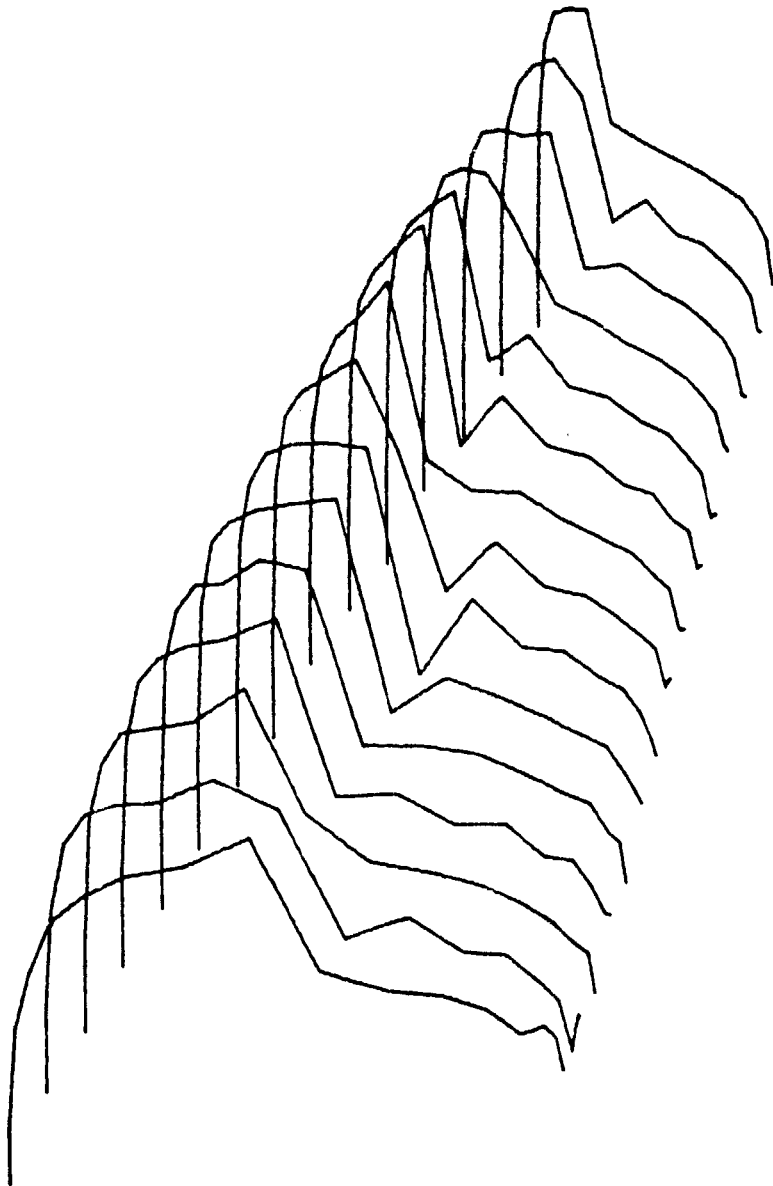
CPO

Fig. 18

CPU

Fig. 19

CR .5

Y

CM −1

Y

Fig. 20

CW .05

Y

Fig. 21

44

XD(Y)
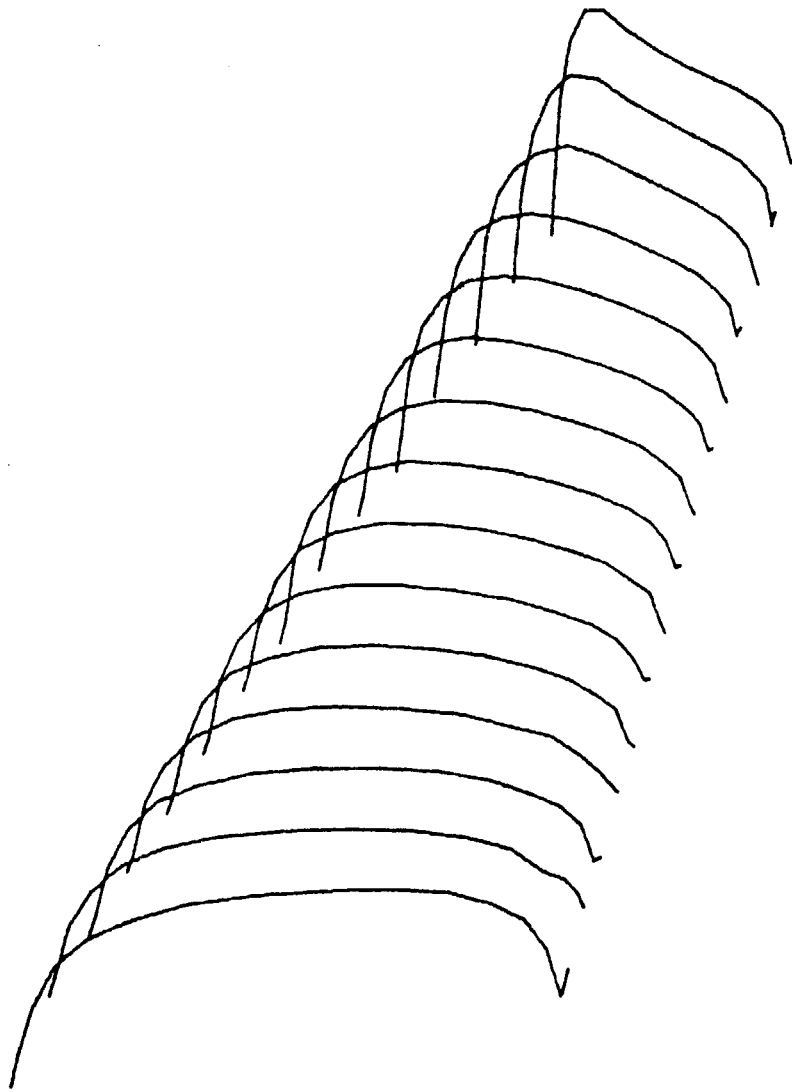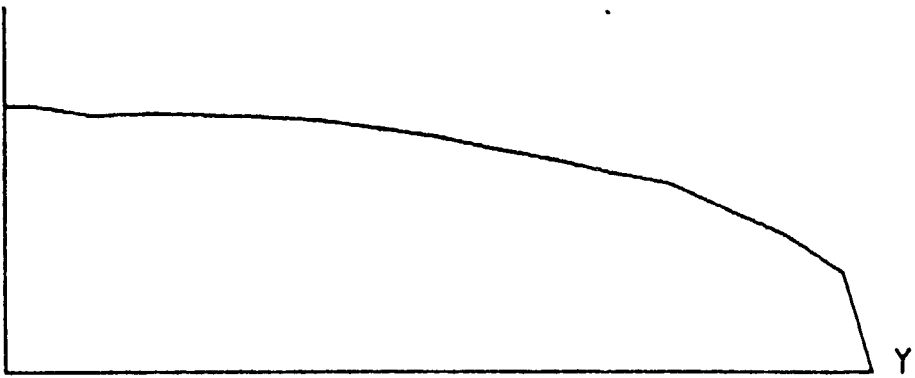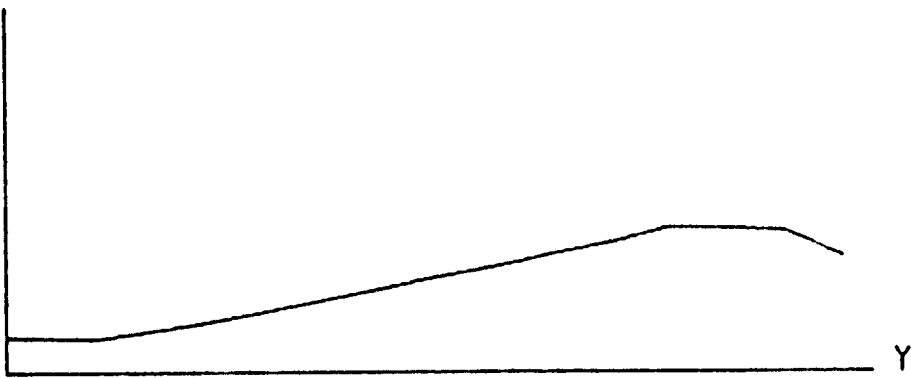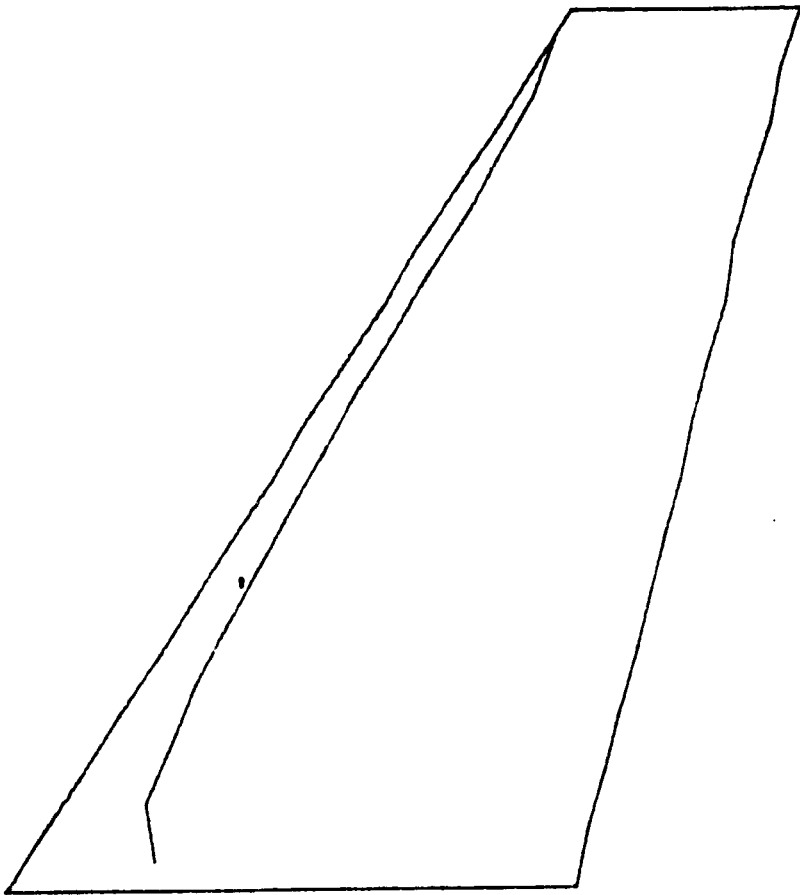
Fig. 22
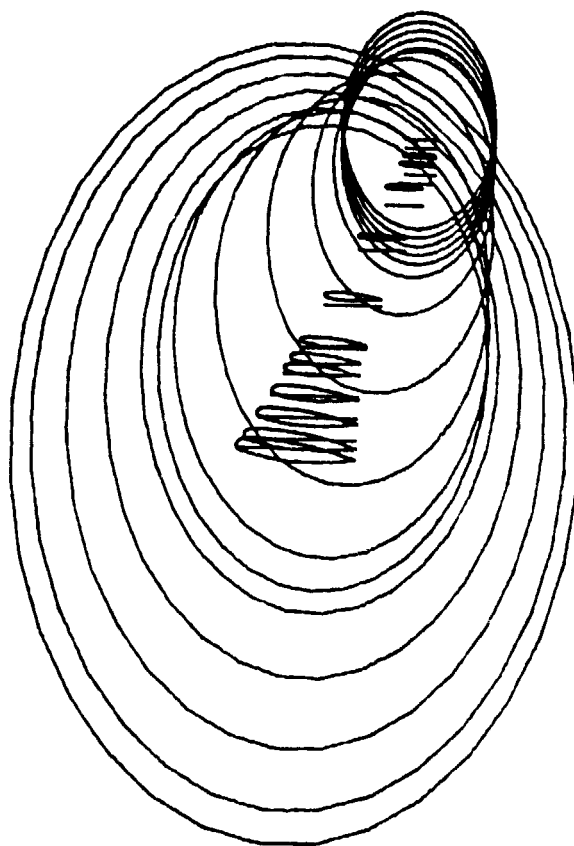
B10X/NLR-   [model]

        [input]

Fig. 23

Y=0.325
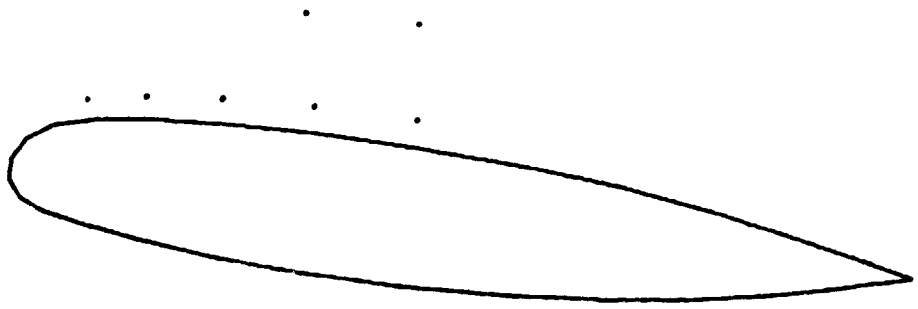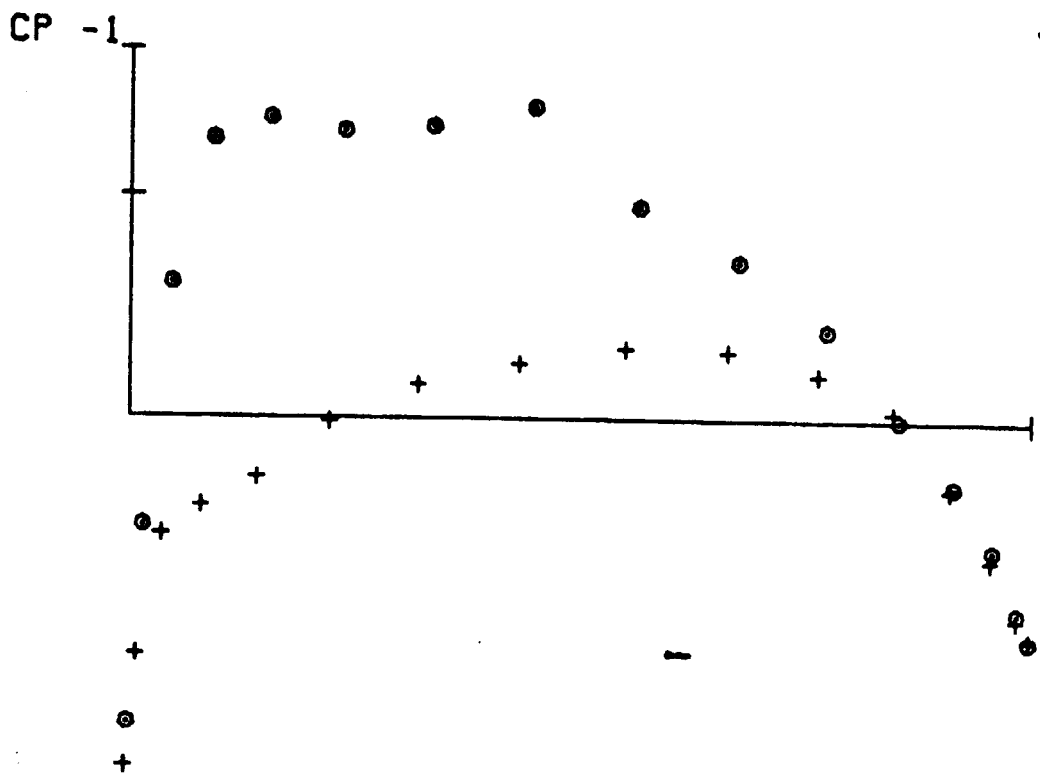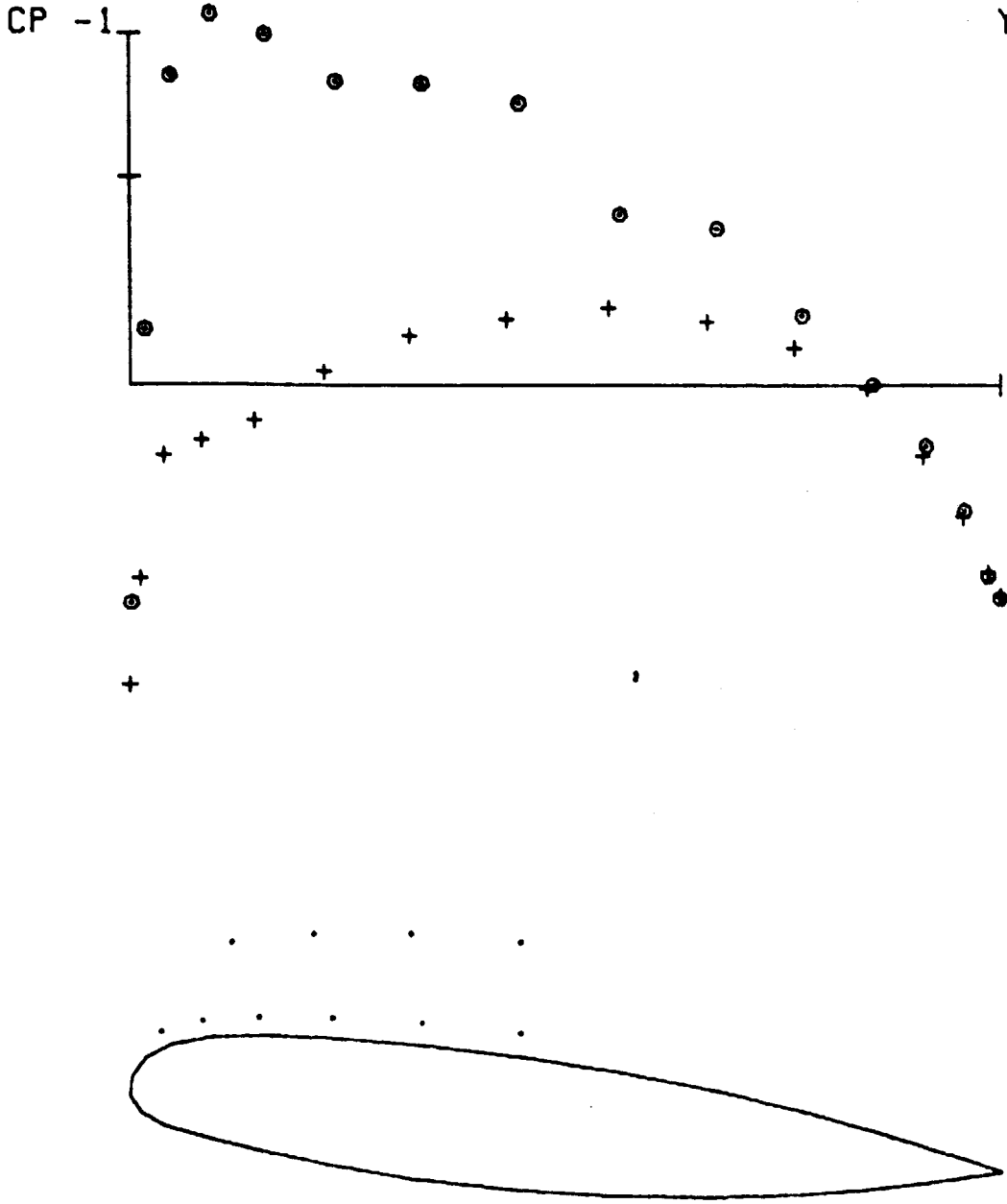
CP -1

Fig. 24

MBB

Y=1.412

CP -1

Fig. 25

Y=2.912

CP -1

Fig. 26

MBB

Y=4.400

CP -1

Fig. 27

MBB

CP -1   Y=5.512

Fig. 28

Fig. 29

CP -1   Y=8.400

Fig. 30

CP −1

Y=11.750

Fig. 31

MBB

Y=15.212

Fig. 32

Y=18.600

/57
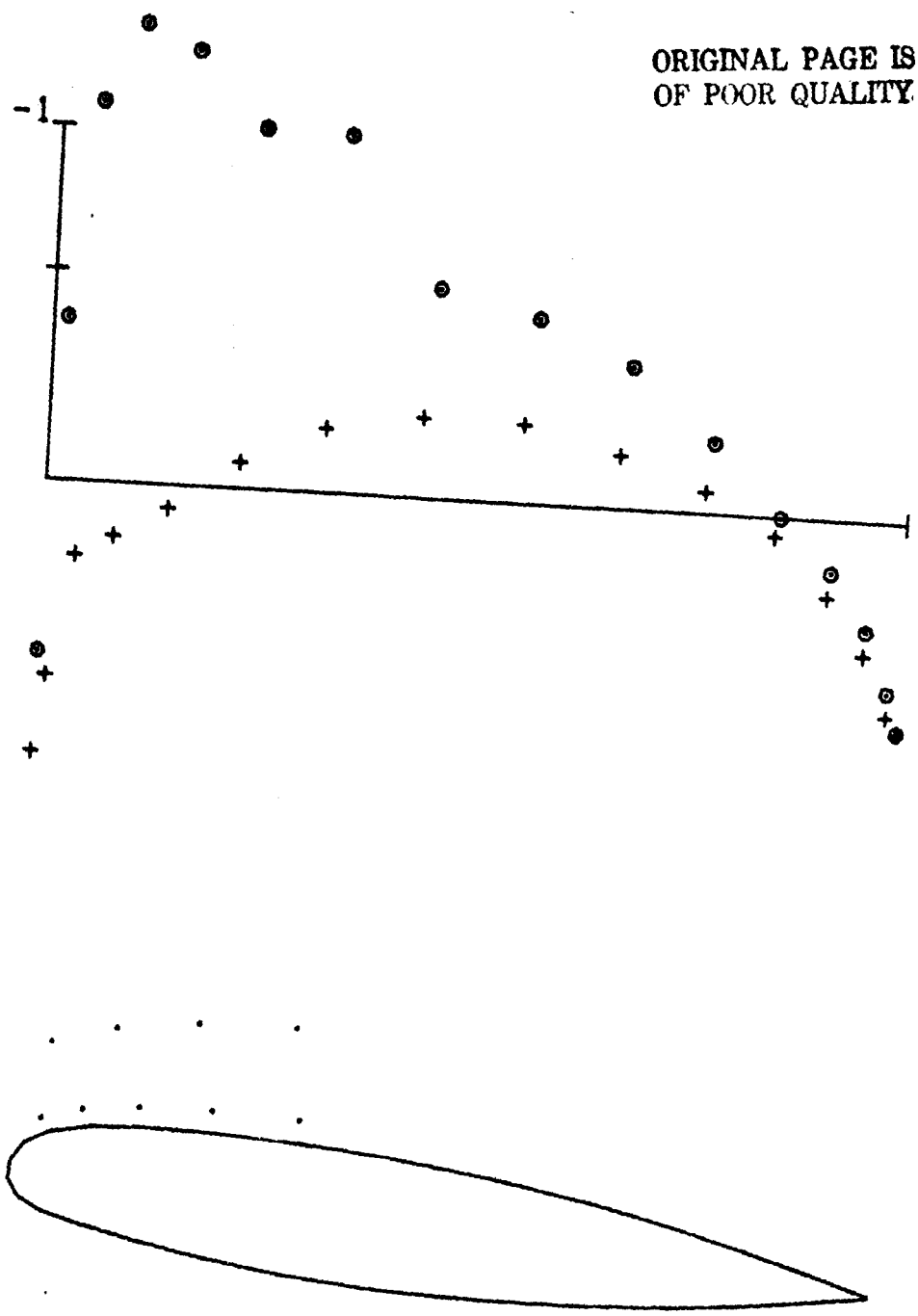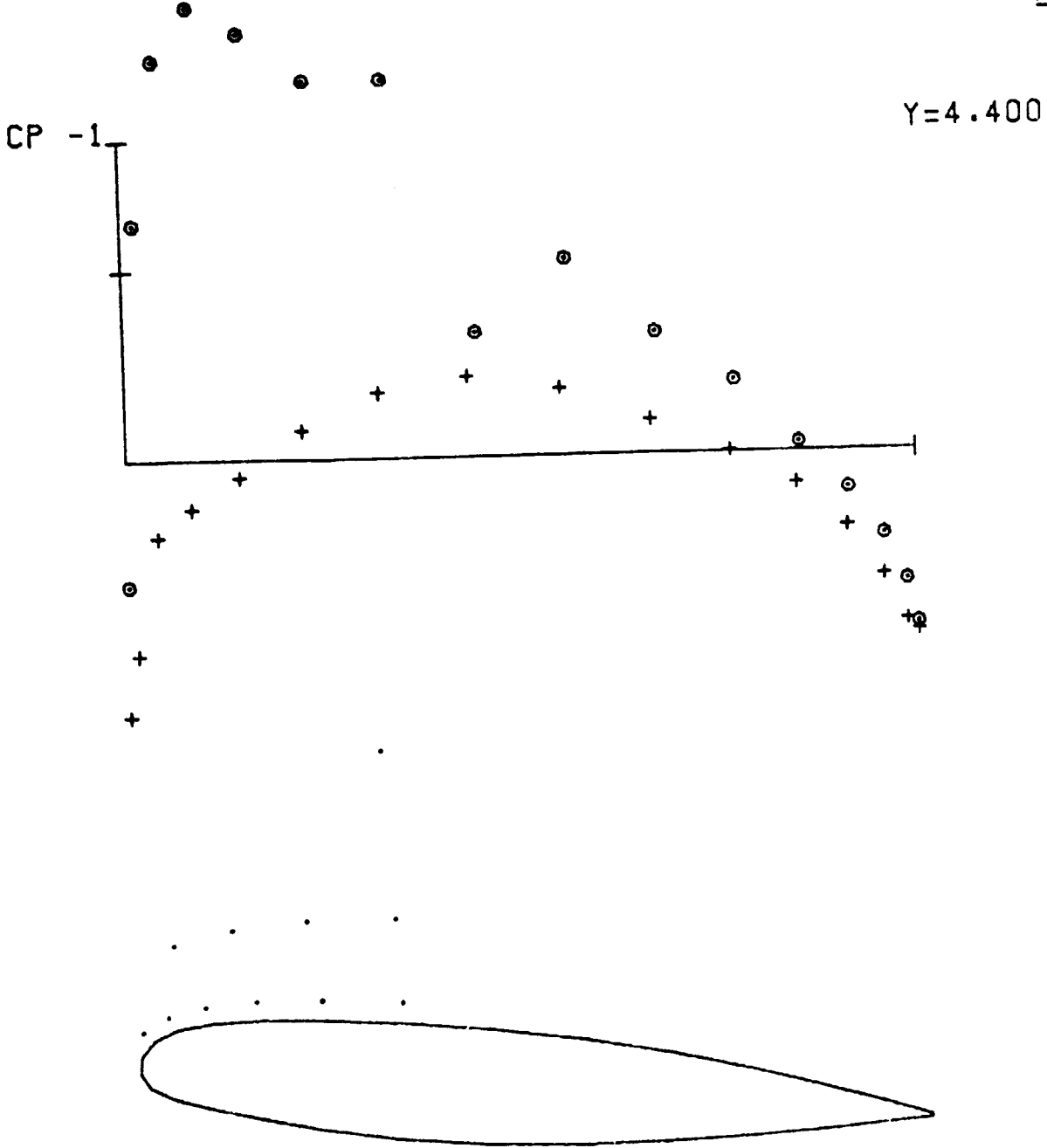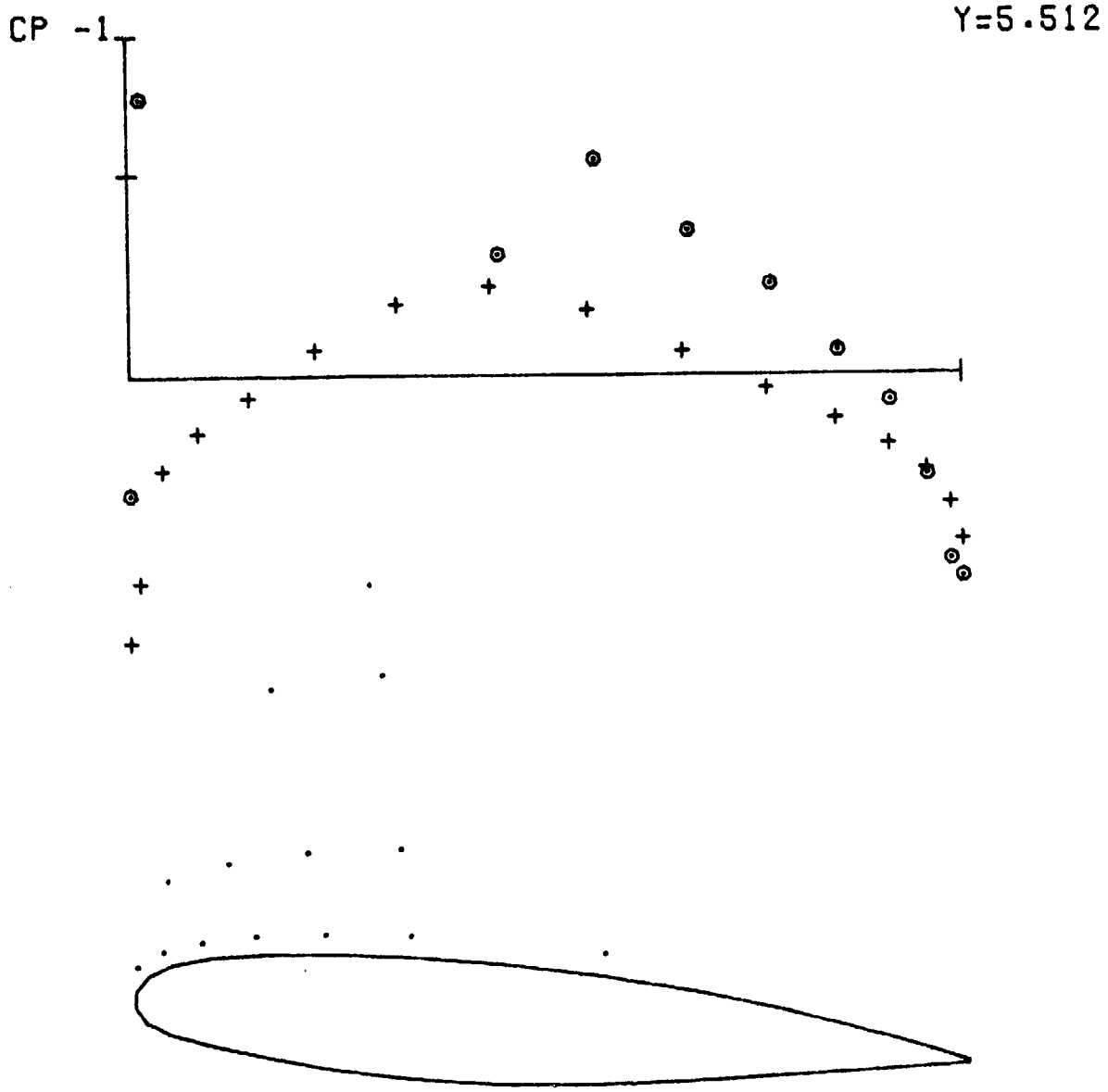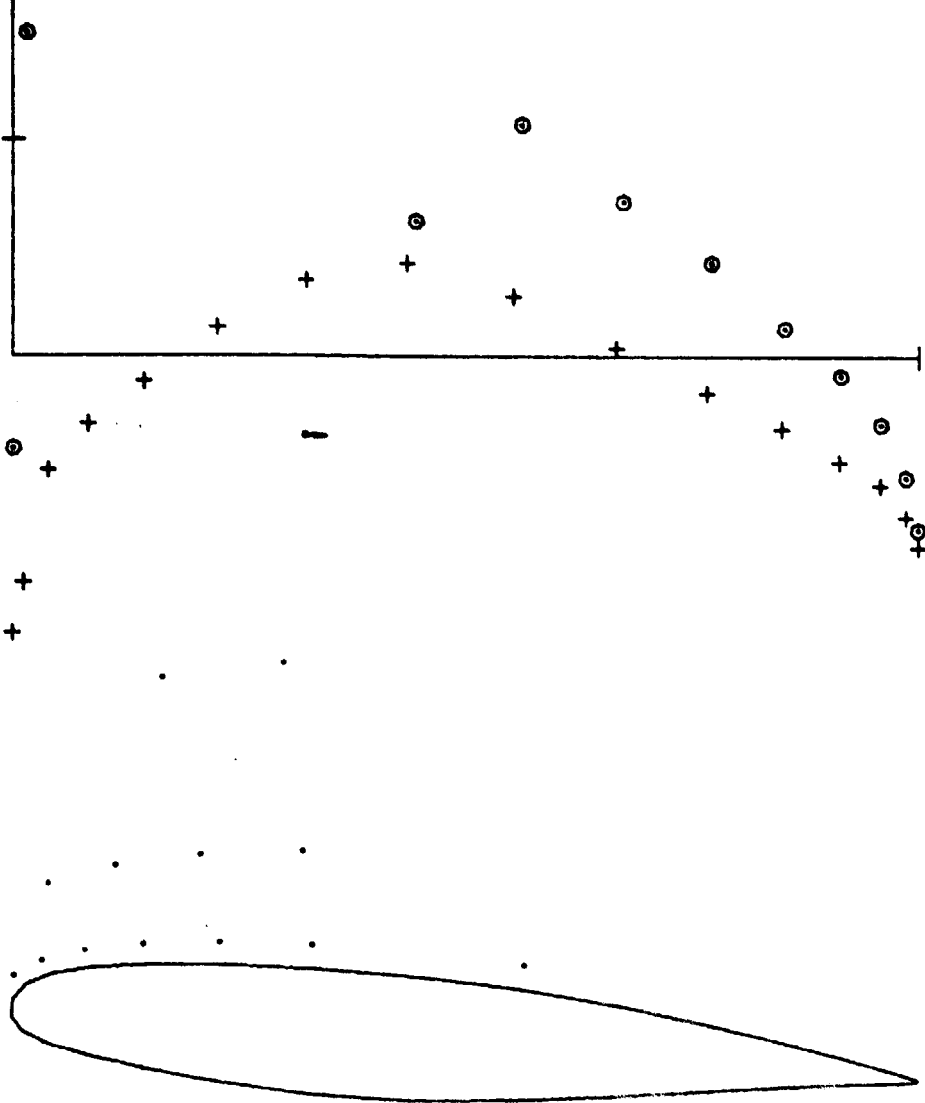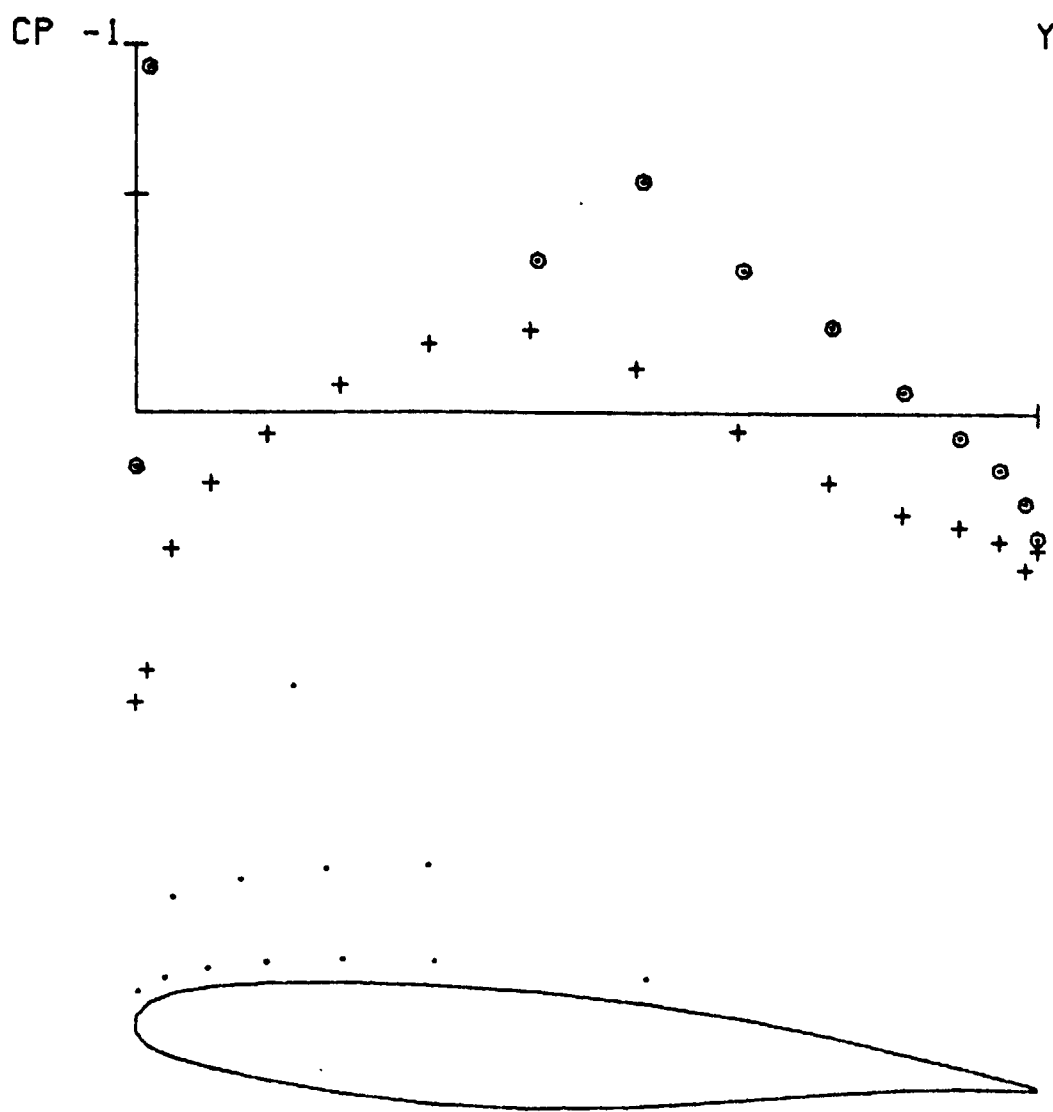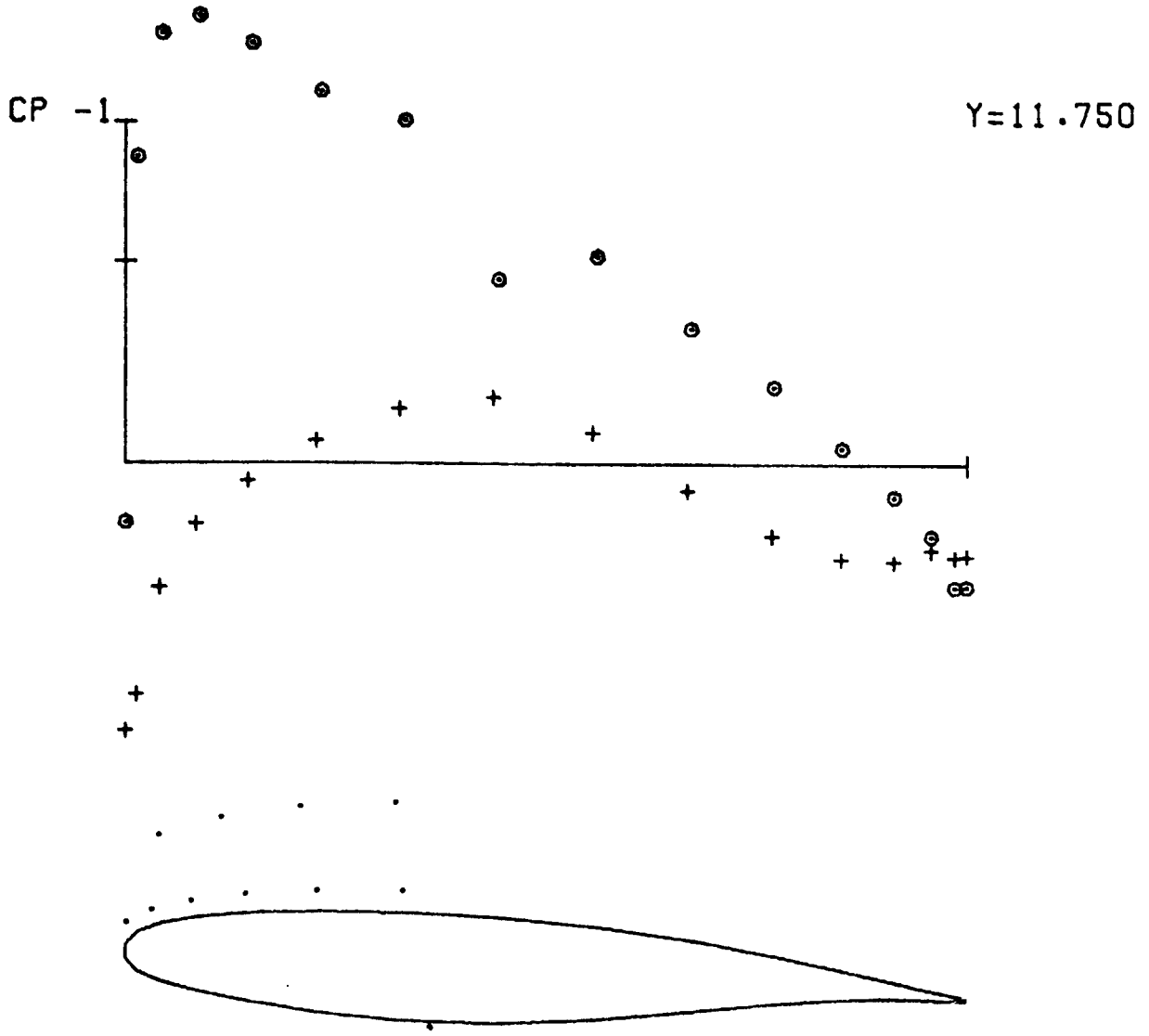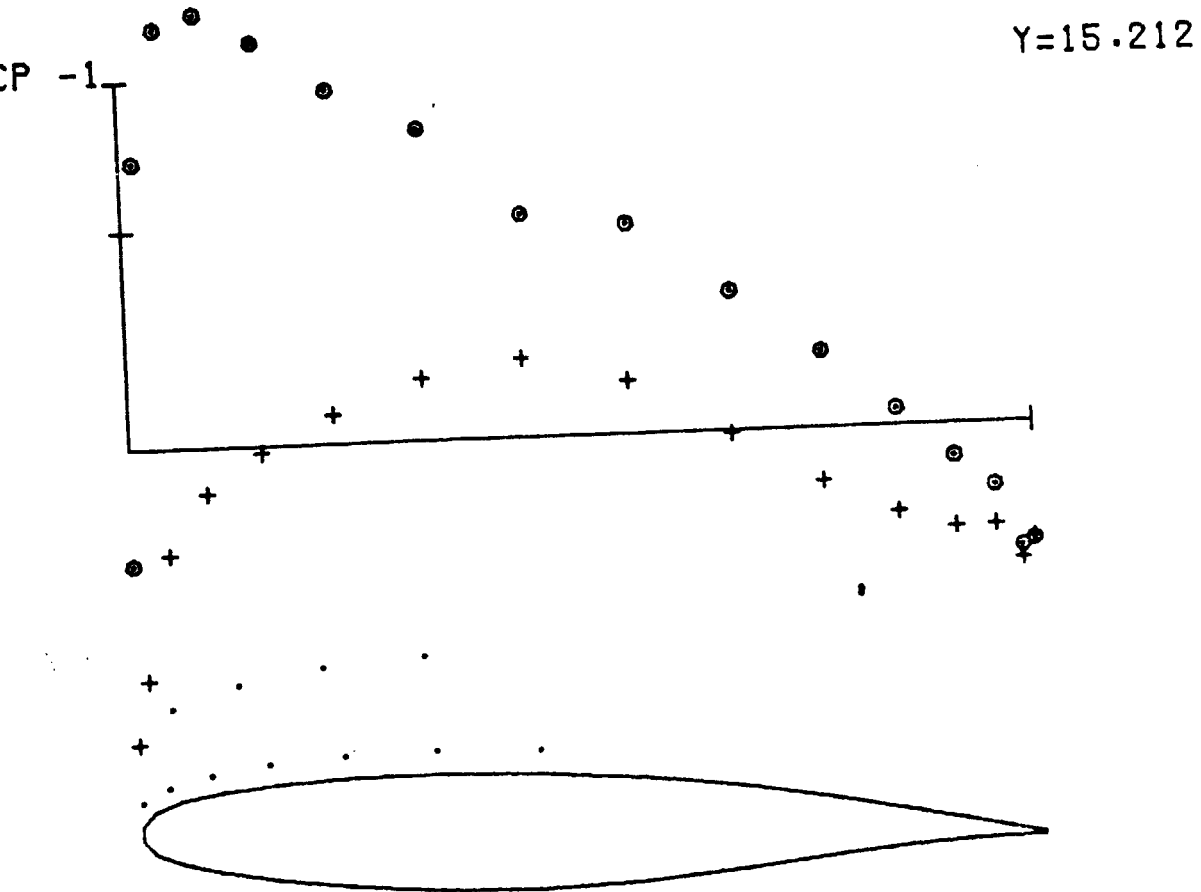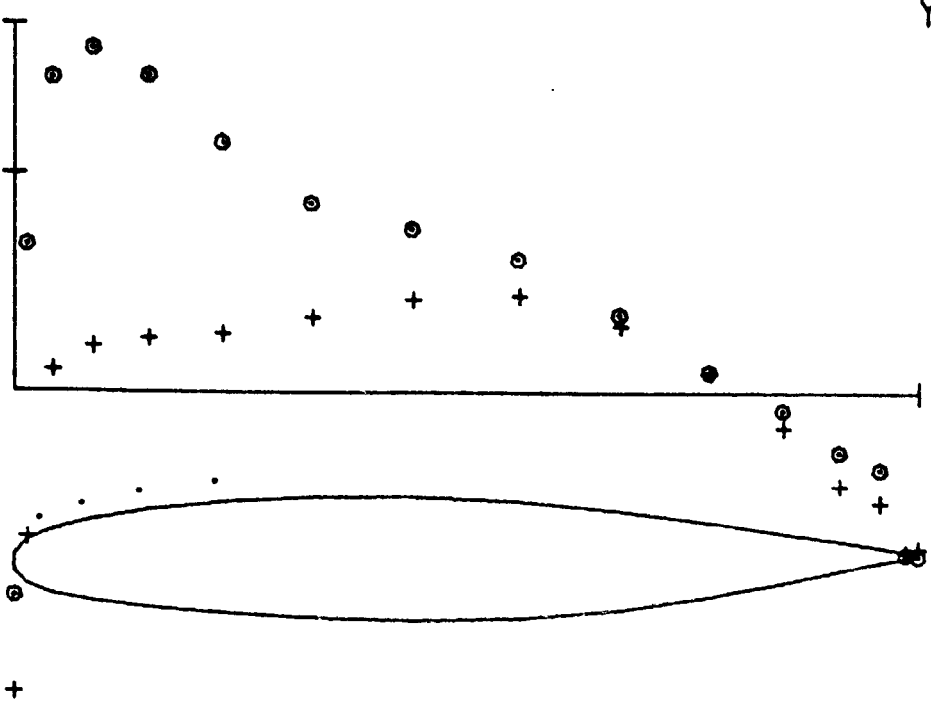
Y=17.537
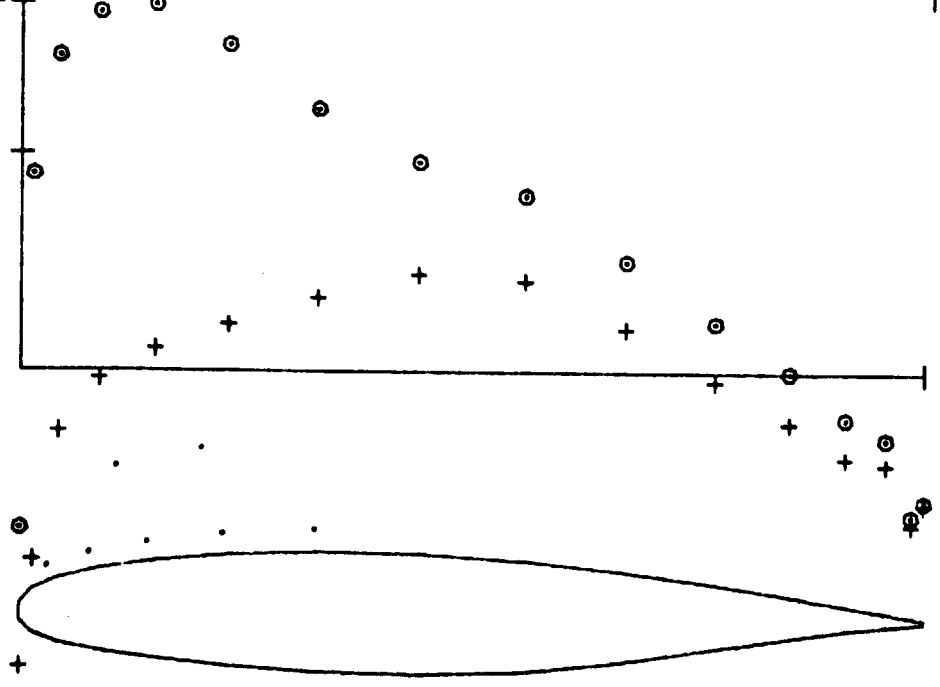
Fig. 33

B10X/NLR-MODELL [model]

MA=0.7500

AL=0.0   GRAD [degree]

BE=0.0   GRAD [degree]

CA=0.5902

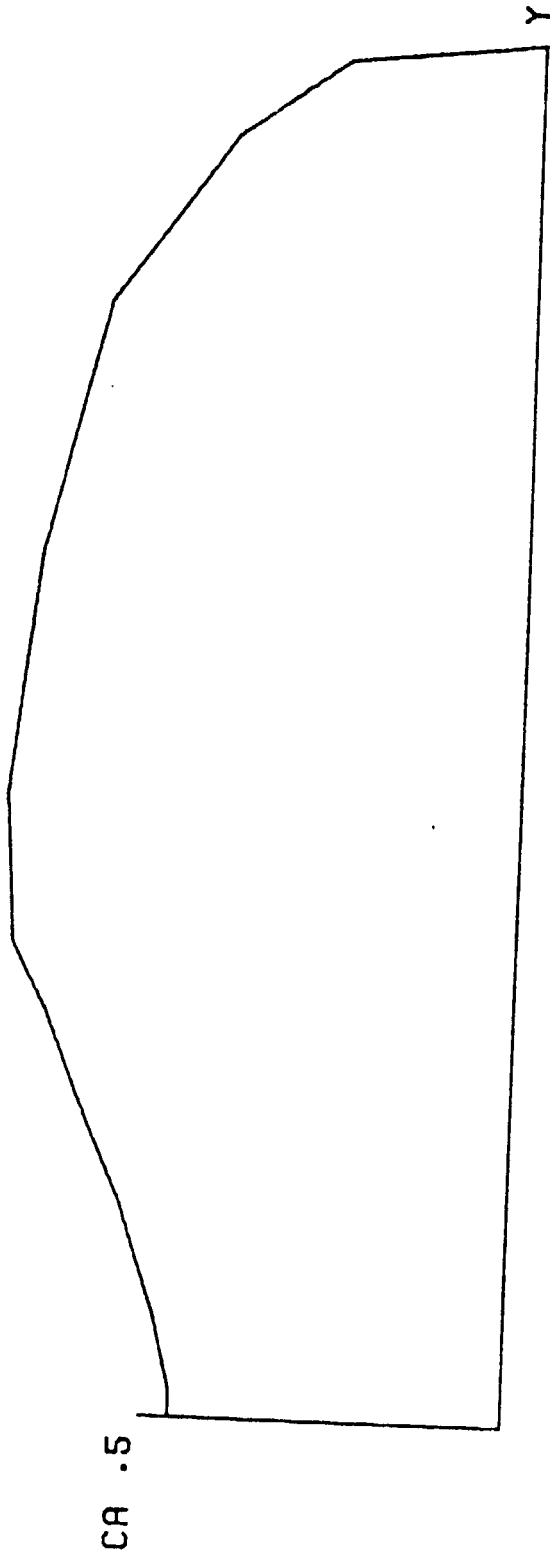CW=0.0305

CM=-0.7258

Fig. 34

CPU   Fig. 35

Fig. 36

CPO

Fig. 37

MBB

Fig. 38

CM .05

Y

Y

CM − .5

Fig. 39

MBB

XD(Y)   Fig. 40

MBB